metals

MDPI

Review

High-Entropy Alloys as Materials for Solid-State Hydrogen Storage: From Fundamental Principles to Directed Design Strategies

Sherzod Kurbanbekov [1,2], Mazhyn Skakov [1], Tolegen Kaisaruly [1], Yulduz Amangeldiyeva [1,2,*], Sherzod Ramankulov [2], Aidyn Tussupzhanov [3] and Yerkhat Dauletkhanov [1]

[1] Center of Excellence "VERITAS", Daulet Serikbayev East Kazakhstan Technical University, Ust-Kamenogorsk 070000, Kazakhstan; sherzod.kurbanbekov@ayu.edu.kz (S.K.); skakov@nnc.kz (M.S.); tkaisaruly@edu.ektu.kz (T.K.); edauletkhanov@edu.ektu.kz (Y.D.)
[2] The Research Institute "Natural Sciences, Nanotechnology and New Materials", Khoja Akhmet Yassawi International Kazakh-Turkish University, Turkestan 161200, Kazakhstan; sherzod.ramankulov@ayu.edu.kz
[3] Nazarbayev Intellectual School of Natural Sciences and Mathematics in Turkestan, Turkistan 161222, Kazakhstan; tussupzhanov_a@trk.nis.edu.kz
* Correspondence: yulduz.amangeldiyeva@ayu.edu.kz; Tel.: +7-778-640-4486

Abstract

High-entropy alloys and the broader class of compositionally complex alloys have recently attracted significant attention as promising materials for solid-state hydrogen storage. Their potential arises not only from high configurational entropy but also from the possibility of tailoring phase composition, crystal structure, local chemical environment, and defect states that govern hydrogen sorption thermodynamics and kinetics. This review summarizes current understanding of hydrogen interaction mechanisms in HEAs and discusses the role of body-centered cubic (BCC), face-centered cubic (FCC), and Laves phases in determining hydrogen capacity, reversibility, and cyclic stability. The limitations of commonly used descriptors, including valence electron concentration (VEC), atomic size mismatch δ, enthalpy of mixing ΔH_{mix}, and Ω parameter, in predicting hydrogen storage behavior are critically analyzed. Particular attention is given to the effects of processing methods, phase transformations during hydrogenation/dehydrogenation, and the energetic heterogeneity of interstitial sites in multicomponent systems. The review highlights that future progress will depend on the transition from empirical alloy discovery toward physically informed multiparametric design integrating CALPHAD, DFT modeling, machine learning, and in situ/operando characterization techniques for the development of efficient and durable hydrogen storage materials.

Keywords: high-entropy alloys; hydrogen storage; BCC; FCC; laves phases; VEC; CALPHAD; DFT; machine learning

Check for updates

Academic Editor: Jiro Kitagawa

Received: 13 April 2026
Revised: 15 May 2026
Accepted: 19 May 2026
Published: 25 May 2026

Copyright: © 2026 by the authors. Licensee MDPI, Basel, Switzerland. This article is an open access article distributed under the terms and conditions of the Creative Commons Attribution (CC BY) license.

1. Introduction

The transition to low-carbon energy systems is increasingly associated with hydrogen as a universal energy carrier capable of enabling the decarbonization of sectors where direct electrification remains difficult. However, the practical realization of the hydrogen economy is determined not only by H_2 production, but also by the safety, energy efficiency, and cost of its storage and transportation [1–3]. Among the existing approaches, including compressed gas, cryogenic liquid hydrogen, and chemical carriers, solid-state hydrogen storage is considered one of the most promising solutions because it provides high volumetric storage

density and allows operation under relatively mild pressure and temperature conditions, thereby potentially improving overall system safety [4–7]. Despite decades of intensive research, the search for materials capable of simultaneously combining high gravimetric and volumetric hydrogen capacity, favorable thermodynamics, fast absorption/desorption kinetics, and long-term cyclic stability remains one of the central challenges of hydrogen technologies [8–10].

Conventional hydride-forming systems possess important advantages; however, each of them exhibits fundamental limitations. Mg-based materials provide high gravimetric hydrogen capacity but require elevated temperatures for reversible hydrogen storage because of unfavorable thermodynamics [11–14]. Solid solutions based on group V elements are characterized by rapid sorption kinetics; nevertheless, they tend to form excessively stable hydrides, which complicates hydrogen desorption and adjustment of the operational P–T window [15–17]. Intermetallic compounds such as TiFe and $LaNi_5$ offer favorable operating conditions and good reversibility, yet they are limited by relatively low storage capacity and/or sensitivity to surface conditions and impurities [18–20]. Consequently, there remains a strong demand for novel solid-state materials with tunable hydrogen storage properties, high cyclic stability, and technological feasibility.

The development of multicomponent alloys has stimulated intensive research into complex concentrated systems, particularly high-entropy alloys (HEAs). Initially, HEAs were regarded as a new class of structural materials formed through multicomponent alloying without a dominant base element [21,22]. However, it later became evident that their potential extends far beyond mechanical applications [23]. Owing to their unique combination of high strength, corrosion resistance, thermal stability, and the possibility of fine-tuning electronic and surface properties, HEAs are also actively investigated for protective coatings, catalysis, electrochemical systems, fuel cells, and battery technologies [23–25]. In particular, considerable attention has recently been devoted to the use of high-entropy alloys as anode materials for nickel–metal hydride (Ni-MH) batteries, where the multicomponent composition enables improvement of electrochemical capacity, cyclic stability, and hydrogen absorption/desorption kinetics compared with conventional intermetallic electrode materials. The vast compositional space, the possibility of forming BCC and FCC solid solutions, Laves phases, and controllable multiphase microstructures have made HEAs promising candidates for hydrogen storage applications [24–26]. Early studies emphasized that the key advantage of HEAs lies not merely in the formal criterion of five elements with concentrations of 5–35 at.%, but rather in the expansion of alloy design principles for multicomponent systems and compositionally complex alloys [27]. As experimental evidence accumulated, it became clear that single-phase solid solutions occur less frequently than originally anticipated, whereas multiphase states are more typical. This led to a transition from the HEA concept toward the broader notion of complex concentrated alloys (CCAs), encompassing chemically complex materials regardless of their microstructural organization [28,29]. Nevertheless, the term “high-entropy alloy” remains the most widely used and recognizable in this field; therefore, it will be employed throughout the present review as the primary term, regardless of the specific microstructural type. The evolution of concepts related to HEAs is schematically illustrated in Figure 1a. As shown in this scheme, the original HEA concept, based on the idea of multicomponent alloying and the core effects, has subsequently undergone substantial reconsideration.

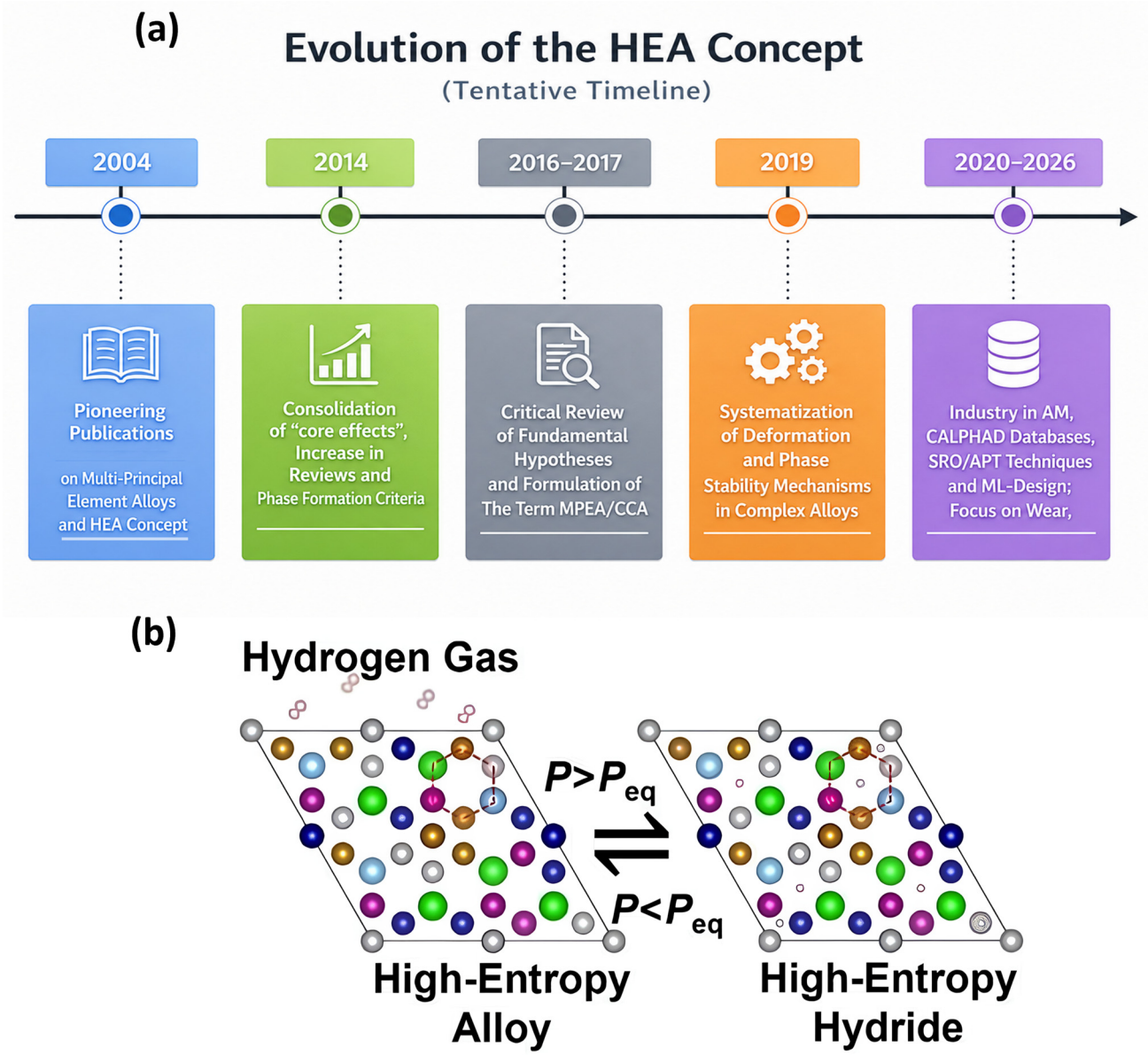


Figure 1. (**a**) Evolution of the HEA concept: from classical high-entropy alloys to compositionally complex alloys and data-driven design; (**b**) The process of interaction of HEAs with hydrogen Reprinted with permission from ref. [29]. 2026 Elsevier.

The interaction of HEAs with hydrogen and the formation of high-entropy hydrides are schematically illustrated in Figure 1b [29]. The colored circles in the scheme represent atoms of different elements constituting the HEA, while their random distribution reflects the chemical disorder characteristic of these systems. The red dashed line schematically indicates the process of hydrogen interaction with the alloy lattice during hydrogen absorption and desorption. This process is reversible and governed by the relationship between the external hydrogen pressure (P) and the equilibrium pressure (P_{eq}). The colored circles in the scheme represent atoms of different elements constituting HEA, while their random distribution reflects the chemical disorder characteristic of these systems. During hydrogenation, hydrogen atoms occupy interstitial sites within the crystal lattice, leading to the formation of a hydride phase. When $P > P_{eq}$, hydrogen absorption and hydride formation occur, whereas at $P < P_{eq}$, the reverse process, namely hydrogen desorption and restoration of the initial alloy state, takes place. Therefore, the equilibrium pressure

is the key parameter defining the conditions for hydrogen sorption and desorption at a given temperature.

A major breakthrough in this field was the report on the TiVZrNbHf alloy, which demonstrated an H/M ratio of approximately 2.5 and a hydrogen storage capacity of about 2.7 wt.% H_2 [30]. This finding was significant for several reasons. First, it showed that multicomponent BCC matrices can exceed the expected performance limits of conventional transition-metal hydrides. Second, it linked the high hydrogen uptake to severe lattice distortion and the complex energetics of interstitial sites. Third, it initiated a series of studies in which HEAs began to be considered not merely as an exotic alloy class but as a distinct platform for the design of hydride materials [30,31].

This review discusses the fundamental aspects of hydrogen interaction with HEAs, including the role of crystal structure and local interstitial chemistry, the limitations of descriptors such as VEC, the influence of synthesis routes on sorption behavior, differences between FCC-, BCC-, and Laves-phase systems, and the prospects of data-driven alloy design. Particular attention is devoted to identifying where HEAs genuinely outperform conventional hydride systems and where the effects of multicomponent alloying remain comparable to traditional factors such as phase composition, microstructure, and defect state.

2. The Reasons for Interest in HEAs as Hydrogen Storage Materials

Historically, discussions surrounding HEAs have been centered on the so-called four core effects: high configurational entropy, severe lattice distortion, sluggish diffusion, and the "cocktail effect" [32,33]. These features, schematically illustrated in Figure 2, distinguish HEAs from conventional alloys in terms of both microstructure and functional properties [34]. For example, in several single-phase FCC [35,36] and BCC [37] HEAs, hydrogen atoms exhibit a lower tendency toward local segregation, thereby improving resistance to hydrogen embrittlement [38]. Compared with single-phase FCC/BCC HEAs, eutectic HEAs forming dual- or multiphase microstructures often demonstrate superior mechanical performance [39]. From a physicochemical perspective, the interest in HEA hydrides is primarily associated with three factors. First, BCC lattices commonly formed in Ti-, V-, Nb-, and Zr-containing HEAs possess a high density of interstitial sites and a favorable geometry for hydrogen storage [40–42]. Second, the local chemical environment of interstitial positions can significantly affect hydrogen–matrix interactions, enabling fine-tuning of sorption behavior [43]. Third, multicomponent systems frequently exhibit hydrogenation-induced phase transformations, tetragonal distortions, crack formation, and self-activation phenomena, which are absent or much less pronounced in conventional binary alloys [44].

In recent years, the behavior of HEA hydrides has increasingly been interpreted in terms of phase constitution, local chemical ordering, and interstitial energetics rather than solely through configurational entropy effects. Consequently, the key challenge is no longer maximizing mixing entropy, but achieving an optimal balance among crystal structure, local chemical order, electronic structure, and the desired thermodynamics of hydride formation [45–49]. Although several HEA systems have already been extensively investigated for hydrogen storage applications [12,50–52], the currently available data still cover only a limited fraction of the enormous compositional space accessible within the HEA paradigm. As shown in Figure 3, most HEAs studied for hydrogen storage are based on transition metals, predominantly Ti, Zr, V, and Nb. Ti, Zr, and V are the most frequently used elements, whereas Cr, Fe, Ni, Mn, and Hf appear less often, and Mg, Al, Ta, Mo, Co, Cu, Ce, and other elements are represented only in a limited number of systems. This distribution indicates that contemporary HEA design for hydrogen

storage is primarily focused on compositions containing hydride-forming elements, while the remaining components are mainly employed to stabilize the structure, control phase constitution, and optimize sorption properties.

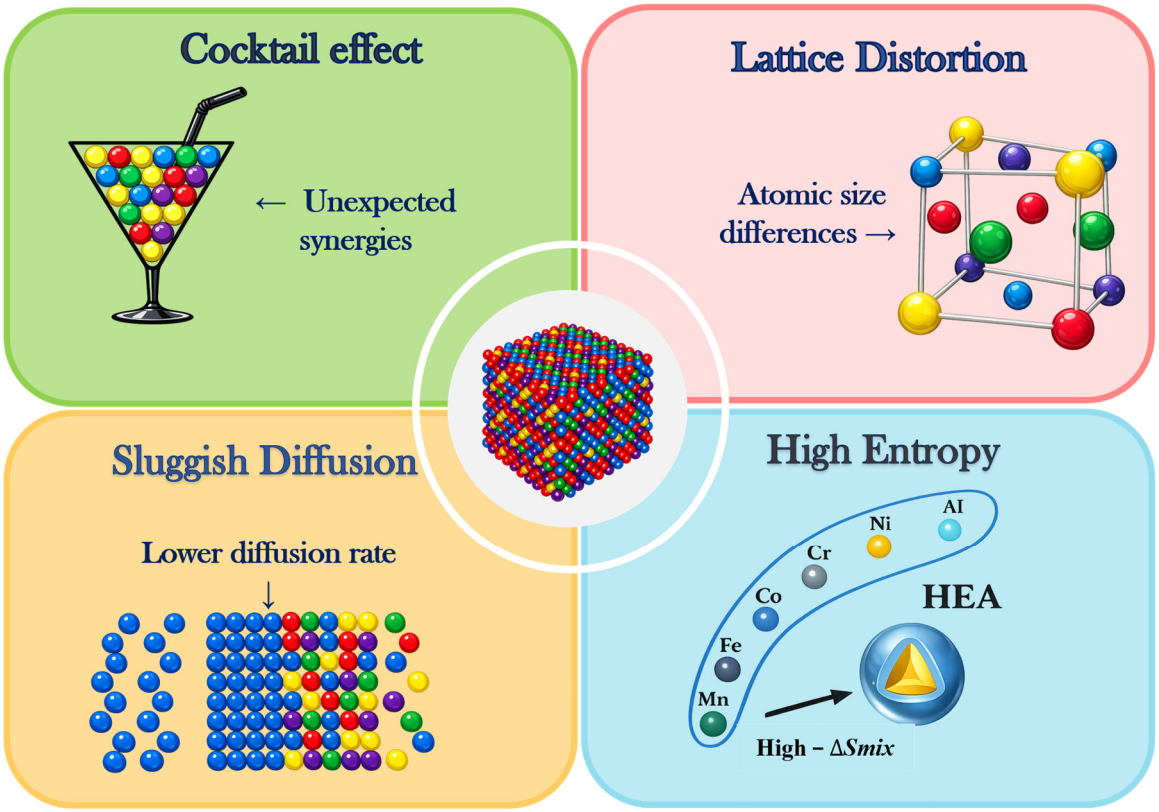


Figure 2. Schematic illustration of the four core effects in HEAs.

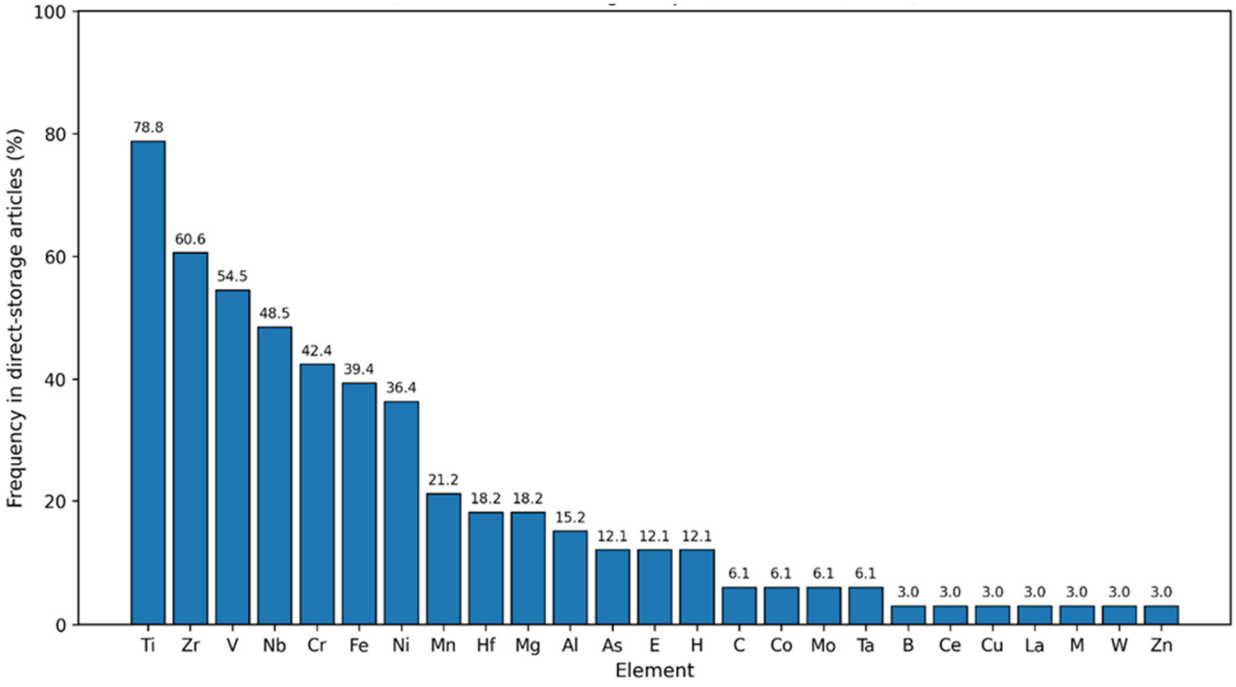


Figure 3. Distribution of Chemical Elements in HEAs Investigated as Hydrogen Storage Materials.

Historically, the selection of elements for hydride-forming alloys has been based on concepts developed in the field of conventional metal hydrides, where the enthalpy of

hydride formation serves as the principal indicator of metal–hydrogen affinity. Within this framework, alloying elements are conventionally divided into hydride-forming (type A) and non-hydride-forming (type B) groups (Figure 4): type A elements are characterized by more favorable (more negative) enthalpies of binary hydride formation and a pronounced tendency to form hydride phases, whereas type B elements thermodynamically suppress hydride formation. Practically, the overall hydrogen affinity of an alloy can be deliberately tailored by combining elements with contrasting hydride formation enthalpies [8,53], and this strategy has accompanied the discovery of several promising HEA compositions for hydrogen storage applications [54,55].

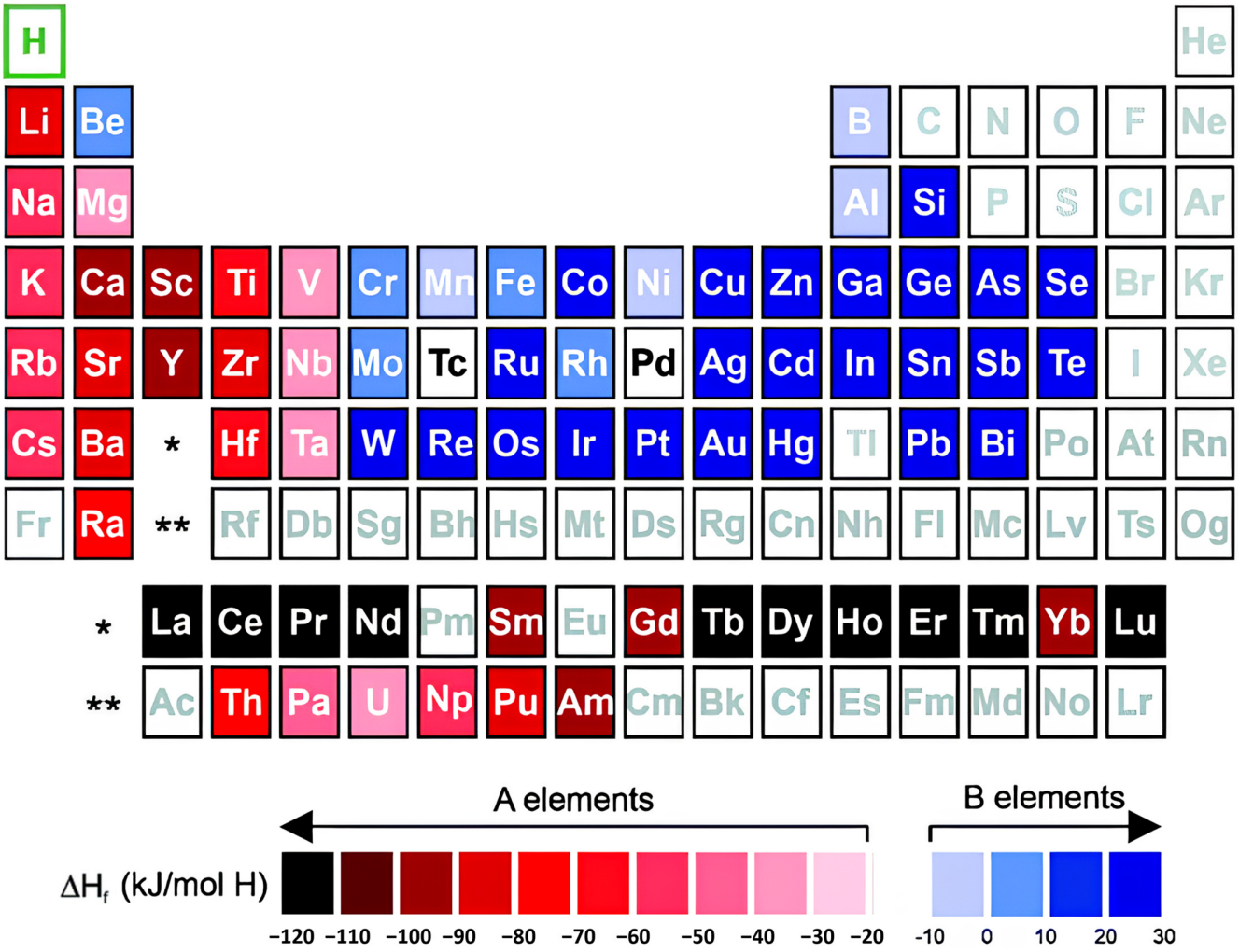


Figure 4. Periodic table showing the relative classification of type A and type B elements based on grouping by the enthalpies of formation of binary metal hydrides. Type A elements are shown in shades of red, type B elements in shades of blue, and hydrogen in green. The symbols * and ** denote lanthanides and actinides, respectively. Reprinted from Ref. [40].

To date, the development of HEAs for hydrogen storage has largely relied on researchers' chemical intuition, as well as on expensive and labor-intensive trial-and-error experiments [56]. At the same time, as will be discussed further, recent years have witnessed the emergence of promising approaches capable of significantly improving the efficiency of alloy design. In this context, critical evaluation of existing composition-selection strategies and their further refinement becomes particularly important for more effective exploration of the still poorly investigated central regions of multicomponent phase diagrams.

3. Structural Factors Governing the Hydrogen Storage Properties of HEAs

HEAs are conventionally classified into three major groups: BCC-dominant alloys with body-centered cubic lattices, FCC systems with face-centered cubic structures, and intermetallic HEAs, including multicomponent Laves phases. This classification is important not only from a crystallographic perspective but also for understanding differences in hydrogen absorption mechanisms, storage capacity, reversibility, and cyclic stability.

The advantage of BCC alloys arises from their high density of interstitial sites and relatively open crystal structure [57]. In conventional Ti-, V-, and Nb-based interstitial systems, BCC matrices have long been considered the most favorable for achieving high H/M ratios. The HEA concept extended this principle to multicomponent systems [58]. Alloys such as TiVNbCrMn, TiVNbCrFe, and Ti-V-Nb-Zr-Cr-Fe demonstrate that appropriate compositional tuning can combine high hydrogen capacity with acceptable activation behavior and notable cyclic stability [59,60]. However, these systems often exhibit the classical trade-off between high hydrogen uptake and excessive hydride stability, which complicates hydrogen desorption [61].

Laves-phase systems represent another important class of hydrogen storage materials. Their main advantage lies not in record hydrogen capacity, but in more predictable and tunable thermodynamics. Multicomponent C14 systems such as Ti-Zr-V-Cr-Ni, TiZrNbFeNi, and AB2-type Zr-based alloys allow adjustment of sublattice composition, thereby controlling plateau pressure, absorption kinetics, cyclic stability, and activation sensitivity [62–64]. FCC systems generally exhibit lower hydrogen capacity than BCC alloys; however, they should not be regarded as secondary. In many HEAs, FCC or pseudo-FCC hydride states form during hydrogenation of the initial BCC matrix, indicating that the FCC phase often represents part of the hydrogen-induced phase transformation sequence rather than an alternative structural state [65].

The formation of specific phase states in HEAs is largely governed by atomic composition, atomic size mismatch, enthalpy of mixing, and configurational entropy. Differences in atomic radii naturally lead to local lattice distortions, thereby affecting the stability of solid solutions and the tendency toward intermetallic or even amorphous phase formation. In this context, several heuristic parameters are widely employed, including the lattice distortion parameter δ, the mixing enthalpy ΔH_{mix}, the configurational entropy ΔS_{mix}, the Ω parameter, the electronegativity difference $\Delta\chi$, and VEC. Their primary value lies in enabling preliminary compositional screening and approximate prediction of phase formation behavior. In general, solid-solution phases are more likely to form at moderate δ values and within a limited range of ΔH_{mix}, whereas increased atomic size mismatch and excessively negative mixing enthalpy promote the formation of intermetallic compounds or amorphous states. The most commonly used empirical and semi-empirical parameters for preliminary prediction of phase formation in HEAs, together with their approximate ranges associated with solid-solution and intermetallic phase formation, are summarized in Table 1.

As shown in Table 1, these parameters enable preliminary compositional screening and estimation of the likelihood of forming solid-solution or intermetallic phases; however, their predictive capability remains limited because of the complex local chemistry and energetic heterogeneity inherent in HEAs.

Table 1. The structural parameters with their formulas.

Parameter	Formula	Range for Solid Solution	Range for Intermetallic	References
ΔS_{mix}	$\Delta S_{mix} = -R\sum C_i lnC_i$	>1.5R		[66]
ΔH_{mix}	$\Delta H_{mix} = \sum_{i=1j\neq 1}^{n} 4c_i c_j \Delta H_{AB}^{mix}$	−15~5 kj mol^{-1}	<0 kj mol^{-1}	[67]
φ	$\varphi = \frac{\Delta S_{mix} - \frac{\lvert\Delta H_{mix}\rvert}{T_m}}{\lvert S_E\rvert}$	>20	\	[68]
Ω	$\Omega = \frac{T_m \times \Delta S_{mix}}{\Delta H_{mix}}$	>1.1	<1.1	[69]
ϕ	$\phi = \frac{\Delta G_{SS} \times \Delta S_{mix}}{-\lvert\Delta G_{max}\rvert}$	>1	\	[70]
δ	$\delta = \sqrt{\sum_{i=1}^{n} c_i \left(1 - \frac{r_i}{\bar{r}}\right)^2} \cdot 100\%$	$\leq$ 6.6%	>3%	[69,71]
$\Delta\chi$	$\Delta\chi = \sum_{i=1}^{n} c_i \left(1 - \frac{\chi_i}{\sum_{i=1}^{n} c_i \chi_i}\right)$	<6%	\	[71–73]
VEC	$VEC = \sum_{i=1}^{N} \{c_i (VEC)_i\}$	$\geq$8.6 for FCC <6.87 for BCC	3.5~8.5	[71,74]

Among these descriptors, VEC occupies a particularly important position and is widely used in HEA research. It serves both as a predictor of the preferred crystal structure and as an indirect indicator of the electronic structure associated with hydride-forming tendencies [75]. In several BCC alloy families, useful correlations between lower VEC values and increased hydrogen capacity have indeed been observed. Nevertheless, the main advantage of VEC is also its principal limitation: it provides only a highly averaged description of the electronic state and does not adequately reflect the real local chemistry surrounding hydrogen atoms, segregation tendencies, secondary-phase formation, or the distribution of interstitial site energies. Consequently, identical VEC values do not necessarily correspond to similar hydride formation enthalpies, plateau pressures, or sorption kinetics. Therefore, VEC should primarily be regarded as a tool for preliminary compositional screening [76].

From a physicochemical perspective, one of the key distinctions between HEAs and conventional binary alloys is the nonequivalence of interstitial sites [77]. Unlike ordered alloys, where hydrogen occupies energetically similar interstitial positions, the chemical and structural diversity of HEAs generates a broad spectrum of energetically heterogeneous interstitial environments [78]. This heterogeneity strongly influences hydride thermodynamics and kinetics, facilitating initial hydrogen absorption, broadening PCT isotherms, promoting hysteresis, and creating deeply trapped hydrogen states that complicate complete desorption under mild conditions [78]. At the same time, it contributes to a more uniform hydrogen distribution, suppresses local concentration oversaturation, and improves cyclic stability during repeated hydrogenation/dehydrogenation.

In this context, comparison of HEA hydrides with conventional hydrogen storage materials is particularly relevant, since each class exhibits its own balance of advantages and limitations (Table 2). AB5- and TiFe-based hydrides provide good reversibility and mild operating conditions but suffer from relatively low gravimetric capacity [79,80]. Mg-based and complex hydrides offer higher hydrogen content, yet require elevated desorption temperatures and additional kinetic optimization [81,82]. Conventional BCC alloys occupy an intermediate position, combining relatively high capacity with acceptable operating conditions, although activation and cyclic stability issues remain significant [83]. Against this background, HEA-based hydrides are regarded as a promising platform due to the pos-

sibility of tuning phase constitution, local chemistry, and hydride thermodynamics through multicomponent alloy design [78]. Nevertheless, their advantages are not yet universal, and current conclusions remain limited by the relatively small number of investigated systems and testing conditions. Therefore, at the present stage, HEA hydrides should be considered a complementary direction in hydrogen storage materials research rather than a complete replacement for conventional hydride systems.

Table 2. Comparison of HEA Hydrides with Traditional Solid-State Hydrogen Storage Systems.

System	H Capacity (wt%)	Advantages	Limitations	Practical Applicability	Ref.
AB5 ($LaNi_5$)	1.2–1.5	Good reversibility, near-room-temperature operating conditions	Low gravimetric capacity due to heavy elements	Mature materials for stationary systems, compressors, and industrial applications; limited by low gravimetric capacity	[79]
TiFe hydrides	1.5–1.9	Good reversibility, moderate operating conditions, low cost	Surface oxidation and hydrogen activation issues; possible kinetic degradation; capacity loss under non-optimal compositions	Attractive for stationary storage and MH-reactors; technologically attractive when activation issues are solved	[80]
Mg-based hydrides	5–7.6	High gravimetric capacity	Difficult activation, slow kinetics and high operating temperatures; catalysts improve stability	Very attractive in terms of theoretical capacity, but limited by kinetics, activation, and temperature regime	[81]
Complex hydrides	5–7	Very high theoretical capacity	Possible phase changes during hydrogenation, kinetic barriers, and thermal effects	Promising for high-capacity systems, but difficult for engineering applications due to complexity and irreversibility of some processes	[82]
Conventional BCC alloys	2–3.8	Operate near room temperature or under moderate conditions; properties tunable via V/Cr/Ti/Mn/Fe composition.	Usually expensive and capacity is often >2 wt.% H_2	Promising for stationary systems and compressors; limited by V cost and long-term stability	[83]
HEA-based hydrides	1.5–3.5	Broad compositional space for tuning thermodynamics, structure, and operating parameters	Experimental data are still limited; possible phase transformations, cracking, and hysteresis changes	Promising platform for further development, but requires standardization, testing, and scale-up	[78]

Alongside metallic hydride systems, lightweight carbon-based materials, including porous carbons, graphene-like structures, and carbon nanotubes, are actively investigated as alternative hydrogen storage media [84]. Unlike HEA-based and conventional hydrides, where hydrogen is mainly stored through interstitial absorption within the crystal lattice, carbon materials primarily rely on physisorption on highly developed surfaces and within microporous structures [85]. Owing to their low density, carbon sorbents exhibit high gravimetric efficiency; however, their best performance is generally achieved at cryogenic

temperatures (~77 K) [86]. At room temperature, the typical hydrogen capacity of most carbon materials remains within ~0.5–2 wt.%, whereas BCC HEAs have demonstrated capacities up to 3.7 wt.% H2 combined with good cyclic stability and reversibility [87]. Furthermore, functionalized graphene-based systems containing metallic centers (Pd, Ni, etc.) may enhance hydrogen storage through spillover and Kubas-like mechanisms, although the reproducibility of such effects still requires further verification [88]. Overall, HEA hydrides appear more promising for stationary and room-temperature hydrogen storage because of their high volumetric density and stability, while carbon-based materials remain particularly attractive for cryoadsorption and hybrid storage systems.

Thus, the hydrogen storage behavior of HEAs is governed not by a single isolated parameter, but by a complex interplay of structural factors, including crystal structure type, degree of local lattice distortion, phase constitution, distribution of interstitial site energies, and the electronic–chemical characteristics of the multicomponent matrix. Consequently, modern HEA design strategies for hydrogen storage increasingly follow a hierarchical multilevel approach: simple heuristics such as VEC, δ, and ΔH_{mix} are first applied for preliminary screening; CALPHAD analysis is then used to evaluate phase equilibria; DFT calculations are subsequently employed to investigate specific interstitial configurations and phase transformation pathways; and, finally, interpretable machine-learning models are introduced for advanced alloy optimization. Such a hierarchical framework represents one of the most realistic pathways for transitioning from empirical alloy discovery toward the rational design of HEA hydrides with a targeted balance of capacity, reversibility, and cyclic durability.

4. Influence of Phase Composition, Hydride Transformations, and Defect Structure on the Sorption Properties of HEAs

The phase constitution of HEAs is one of the key factors governing their interaction with hydrogen. For solid-state hydrogen storage systems, maintaining the phase stability of the initial matrix and understanding structural evolution during hydrogen absorption and desorption are of particular importance [89–95]. The crystal structure type, presence of secondary phases, interphase boundaries, and defect subsystem play especially significant roles, as they determine the available interstitial sites, hydrogen insertion energetics, migration pathways, and degradation mechanisms during cyclic operation [96–100].

Solid-solution states, particularly BCC matrices, are generally considered the most favorable structural basis for achieving high hydrogen capacity and acceptable sorption kinetics [101]. In BCC lattices, hydrogen mobility is typically higher than in FCC systems because of the geometry of interstitial sites and lower migration energy barriers [102]. However, structural homogeneity is important not only from the perspective of diffusion. A single-phase matrix provides more predictable hydrogen distribution, reduces chemical heterogeneity, and lowers the probability of local hydrogen accumulation that may induce internal stresses and accelerated degradation. In contrast, multiphase structures amplify the influence of interfaces, secondary phases, and local compositional fluctuations, resulting in more complex and often less reproducible sorption kinetics [103,104]. In this context, phase-formation criteria such as Ω and δ are valuable not as independent descriptors, but rather as tools for controlling structural homogeneity required for long-term cyclic stability [105].

Crystal defects also strongly influence hydrogen storage behavior. Dislocations, grain boundaries, interphase interfaces, and local elastic stresses form a multilevel network of hydrogen trapping centers. On the one hand, such defects may accelerate initial absorption by increasing the number of energetically favorable sites and facilitating local hydrogen penetration into the material [106]. On the other hand, they may promote local hydrogen

accumulation, stress concentration, hysteresis, and enhanced embrittlement susceptibility [107]. Consequently, the defect subsystem plays a dual role, simultaneously broadening the spectrum of hydrogen-interaction mechanisms while complicating the achievement of stable reversibility during cycling. This issue is particularly critical for HEA hydrides, where intrinsic chemical and size-related disorder already creates a broad distribution of local trapping sites, and structural defects further amplify this heterogeneity [108,109].

One of the central questions concerns the hydrogenation pathway of BCC-dominant HEAs [110]. Similar to many conventional BCC alloys, these materials commonly form a monohydride phase and, under certain conditions, may further transform into a dihydride phase (Figure 5). In a single-stage mechanism, hydrogen absorption proceeds mainly through monohydride formation without subsequent dihydride transformation, resulting in high reversibility and improved cyclic stability, although typically at the expense of maximum hydrogen capacity. In a two-stage mechanism, the initial formation of a BCC (or slightly distorted BCC/BCT) monohydride is followed by transformation into an FCC dihydride phase, which may increase hydrogen capacity but also complicates the kinetics and reaction conditions.

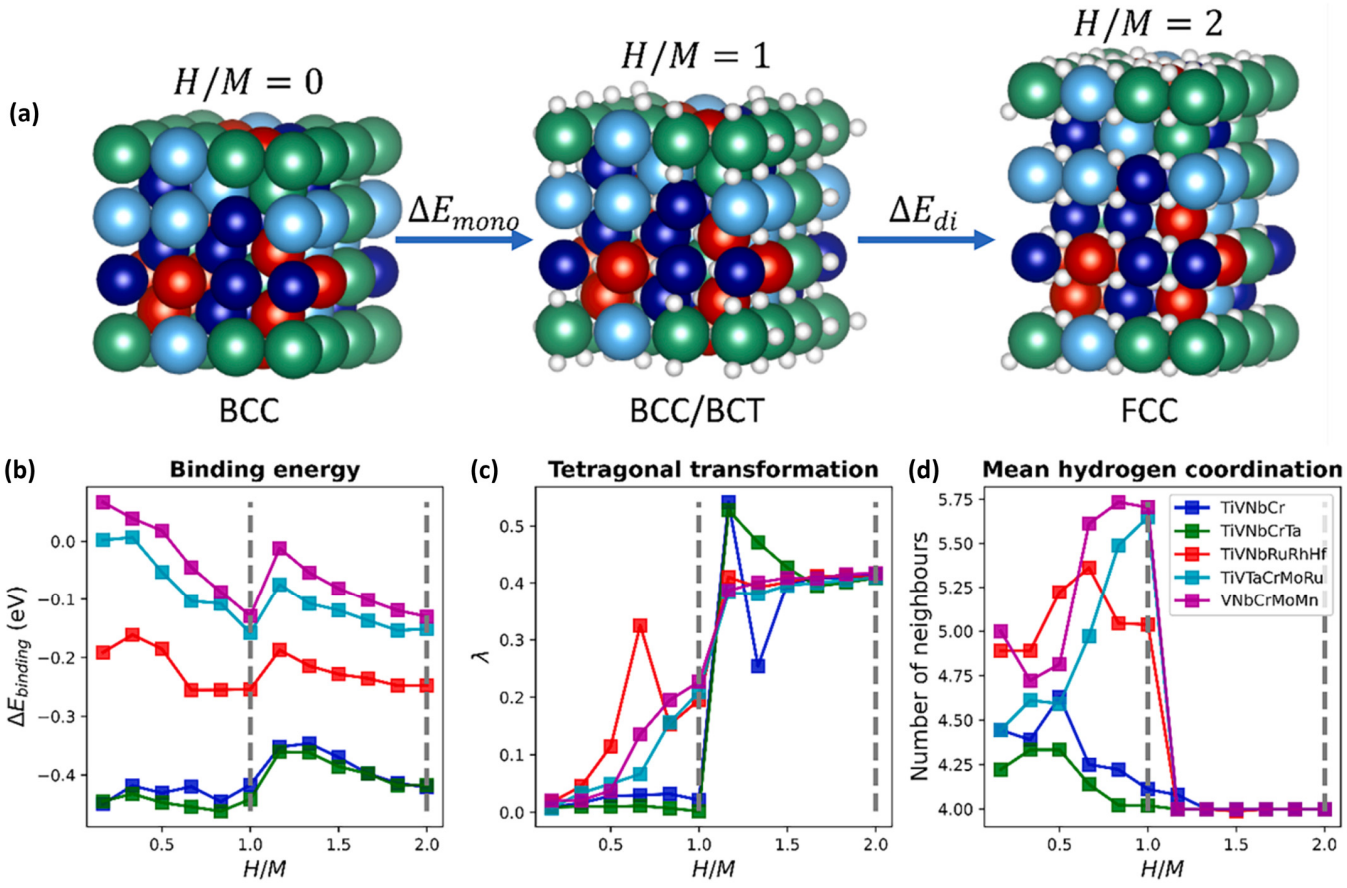


Figure 5. Schematic representation of the computational approach used to analyze hydrogen interaction with high-entropy alloys: (**a**) general DFT-based scheme for determining hydrogen binding energy, where the small white spheres correspond to hydrogen atoms and the large colored spheres represent metal atoms; (**b**) hydrogen binding energy; (**c**) tetragonal structural transformation of the lattice; (**d**) average coordination environment of hydrogen for five selected high-entropy alloys. Reprinted from Ref. [110].

A representative example is the TiZrNbHfTa alloy investigated by Cristina Zlotea and co-workers [30]. In situ X-ray diffraction revealed a two-stage desorption mechanism in this system: significant hydrogen release began at approximately 180 °C and was accompanied by the formation of a monohydride phase, whose fraction reached a maximum near 200 °C and subsequently decreased, while further heating gradually restored the initial BCC matrix. During short accelerated cycling, only the reversible response associated with the monohydride phase was observed, whereas the dihydride phase did not have sufficient time to form to a significant extent. These results demonstrate the strong sensitivity of hydride transformations to the lattice distortion parameter δ. Variations in δ modify the energetic landscape of phase transformations and therefore affect the balance among hydrogen capacity, reversibility, and reaction kinetics.

Analysis of BCC alloys has further shown that the valence electron concentration (VEC) may correlate not only with the type of metallic crystal structure, but also with the stability of hydride phases [111]. In particular, it has been reported that above a threshold value of approximately VEC ≈ 4.75, thermodynamic destabilization of dihydride states occurs, thereby facilitating hydrogen release [112]. At lower VEC values, hydrogen capacities approaching ~2 H/M become achievable, whereas the best compromise between high capacity and acceptable cyclic stability is typically observed within a relatively narrow VEC range of 4.75–5.0 [113]. With a further increase in VEC, the maximum hydrogen capacity generally decreases. These observations confirm that electronic factors play an important role in determining the sorption behavior of BCC HEAs [114], although the overall response also depends strongly on phase constitution and local structure.

Thus, the hydrogen storage performance of HEAs is governed not merely by their classification as BCC-, FCC-, or Laves-type systems, but primarily by the specific architecture of their phase constitution and defect structure, which evolve during hydrogenation. Single-phase BCC matrices generally provide higher hydrogen capacity and improved diffusion but may suffer from excessive hydride stability and difficult desorption. In contrast, multiphase and intermetallic systems typically exhibit lower maximum capacity, yet often offer more controllable thermodynamics and enhanced cyclic stability. Defects, interphase boundaries, and the nonequivalence of interstitial sites further modify both kinetics and reversibility. Consequently, the design of HEAs for hydrogen storage should focus not on identifying an abstractly "optimal" structure type, but rather on achieving the best balance among phase stability, hydrogen capacity, desorption behavior, and resistance to cyclic degradation.

5. Influence of Processing Route and Microstructure

Synthesis and processing technologies play a crucial role in determining the microstructure of HEAs for hydrogen storage, emphasizing the importance of selecting appropriate fabrication routes [53,115]. Arc melting remains the dominant method in the HEA-hydride literature because it enables rapid production of cast ingots and efficient screening of new compositions (Figure 6a). However, the as-cast state often retains dendritic and interdendritic chemical heterogeneity, coarse grains, and sorption behavior strongly dependent on subsequent crushing and activation procedures.

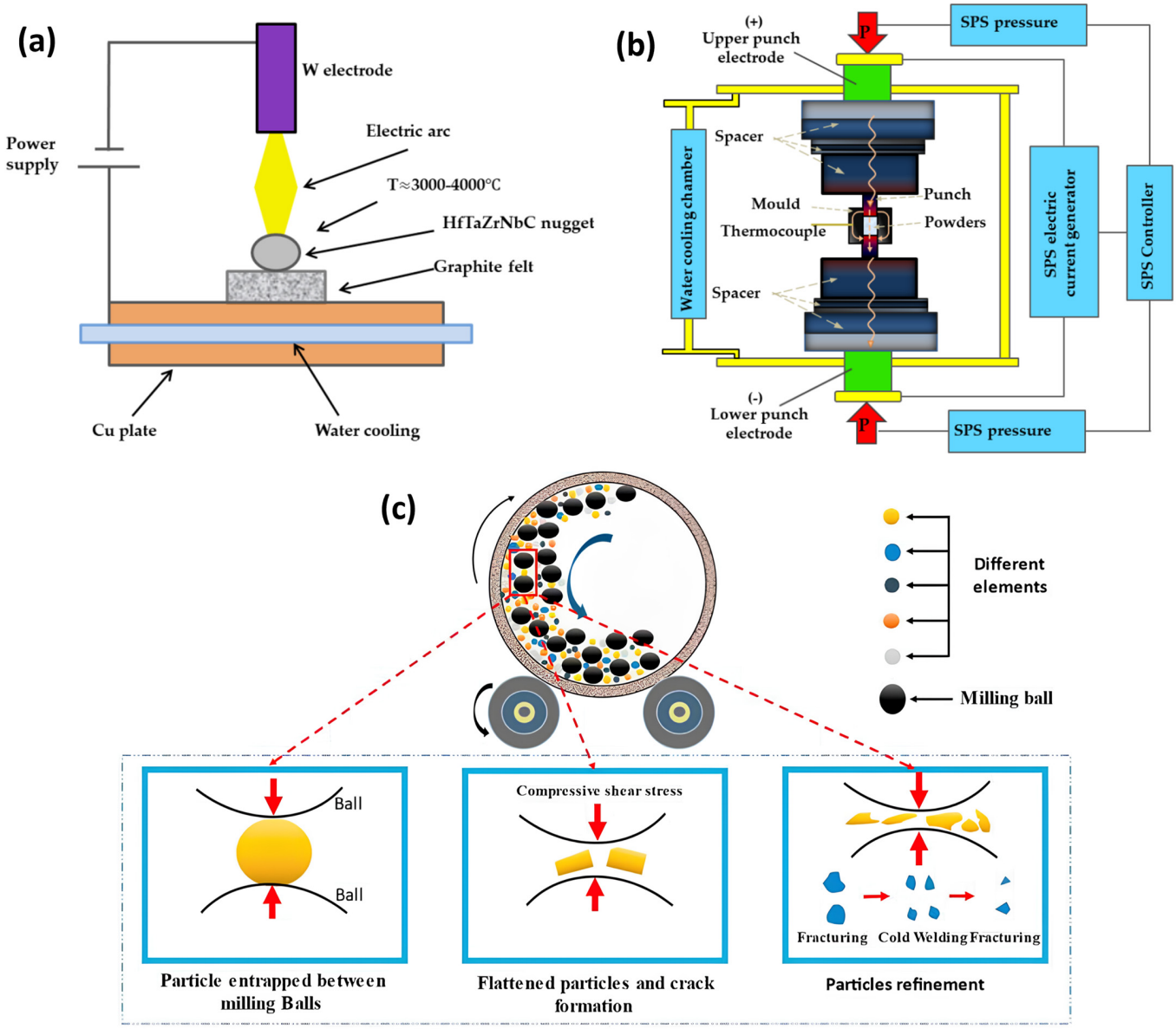


Figure 6. Schematic representation of the main processing routes for the fabrication of HEAs: (**a**) arc melting [116], (**b**) spark plasma sintering [117], and (**c**) mechanical alloying/high-energy ball milling. Reprinted from Ref. [118].

Powder metallurgy represents one of the most important approaches to improving alloy processing efficiency, particularly for high-entropy hydrogen storage materials, as it combines powder production with subsequent consolidation by sintering [118,119]. Among powder fabrication techniques, mechanical alloying and high-energy ball milling are the most widely used, since they produce finer, defect-rich, and often more chemically homogeneous microstructures at small length scales. These methods also introduce large numbers of dislocations, grain boundaries, and nonequilibrium states, which may facilitate initial hydrogen sorption. Additional powder production routes, including atomization and electrolytic powder synthesis, are also employed. During powder consolidation, several major sintering techniques are applied, including liquid-phase sintering, hot pressing, activated sintering, and spark plasma sintering (SPS) [120]. Among these, SPS is of particular interest because it enables precise microstructural control of HEAs, which is critically important for targeted optimization of hydrogen sorption properties (Figure 6b) [121].

Laser deposition is another promising route for the synthesis of HEAs for hydrogen storage due to its capability for continuous material addition [122]. The most common approach is laser engineered net shaping, implemented within computer-controlled systems with predefined processing parameters [122]. The use of different powder-feeding mechanisms and nozzle configurations allows precise adjustment of powder flow and alloy composition.

For a systematic comparison of the main synthesis and processing routes employed in hydrogen-related HEA research, Table 3 summarizes the key technological parameters, typical microstructural risks, and rational application areas of different processing approaches.

Table 3. Methods for HEA fabrication/processing and key control parameters.

Route	Key Processing Parameters	Typical Microstructural Risks	Main Advantages/When to Choose
Casting (arc/induction melting, vacuum melting, etc.)	purity, cooling rate, homogenization, mixing	dendritic segregation, shrinkage defects, coarse-grain size	rapid composition screening; compatibility with conventional metallurgy; convenient for EHEAs
Powder metallurgy: MA + SPS	MA energy/time, atmosphere, PCA, SPS conditions (T-P-t)	O/N/C contamination, porosity, nonequilibrium phases, residual stresses	production of fine-grained/lamellar structures; effective for RHEAs and complex systems
Additive manufacturing (LPBF/L-PBF, DED/L-DED, binder jet, WAAM)	beam energy, scanning speed, strategy, preheating, powder characteristics	porosity, cracking, evaporation/loss of volatile elements (for example, Mn), nonequilibrium phases	complex geometry; local microstructure control; potential for gradient materials and coatings
Heat treatment (homogenization/aging/annealing)	temperature, time, cooling rate	decomposition of solid solutions, grain growth, σ/Laves precipitation	key route for precipitation strengthening ($L1_2$/B2) and phase stabilization
SPD (HPT, etc.)	strain, pressure, temperature, number of revolutions	instability upon heating, corrosion changes, anisotropy	extreme grain refinement; study of grain-boundary effects, single-phase stability, and deformation mechanisms

As shown in Table 3, the same HEA composition may develop substantially different phases and microstructural states depending on the processing route, which directly affects activation behavior, sorption kinetics, and cyclic stability. Therefore, the discussion of HEAs for hydrogen storage cannot be limited to alloy composition and measured hydrogen capacity alone. At a minimum, information regarding the synthesis route, phase constitution before and after hydrogenation, particle morphology, activation procedure, and cycling history is required. Without such data, comparison of materials reported in different studies becomes highly conditional, and broader conclusions remain unreliable.

The mechanistic relationship between processing route, microstructure, and hydrogen storage behavior in HEAs has been confirmed by XRD, SEM/EDS, XPS, and FTIR investigations of various systems. These studies demonstrate that variations in grain size, phase constitution, defect density, and interphase boundaries formed during processing directly influence hydrogen absorption mechanisms, lattice parameters, phase transformations, and hydride cyclic stability.

For example, Park and co-workers showed that SPS processing of the refractory HEA TaNbHfZrTi at 1100 °C produced a homogeneous fine-grained BCC structure (~22.5 μm compared with ~228 μm in the cast alloy) [123]. After hydrogenation, XRD analysis revealed destabilization of the initial BCC lattice and partial formation of HCP hydride phases, accompanied by peak broadening and shifts in the BCC reflections toward lower 2θ angles. These changes indicate lattice expansion caused by hydrogen insertion and the formation of a more heterogeneous two-phase structure consisting of BCC and HCP hydride phases.

For the arc-melted $TiV_2ZrCrMnFeNi$ alloy, combined PCT, kinetic, and XRD analyses demonstrated that C14/BCC interphase boundaries strongly affect sorption behavior [124]. After hydrogenation, the volume fraction of the C14 Laves phase increased by approximately 15%, while its lattice parameters expanded to a = b = 0.519 nm and c = 0.849 nm. XRD results confirmed preferential hydrogen localization within the C14 phase, whereas the lattice parameter of the BCC phase remained nearly unchanged (Figure 7). Importantly, the alloy retained stable performance over at least 50 hydrogenation/dehydrogenation cycles.

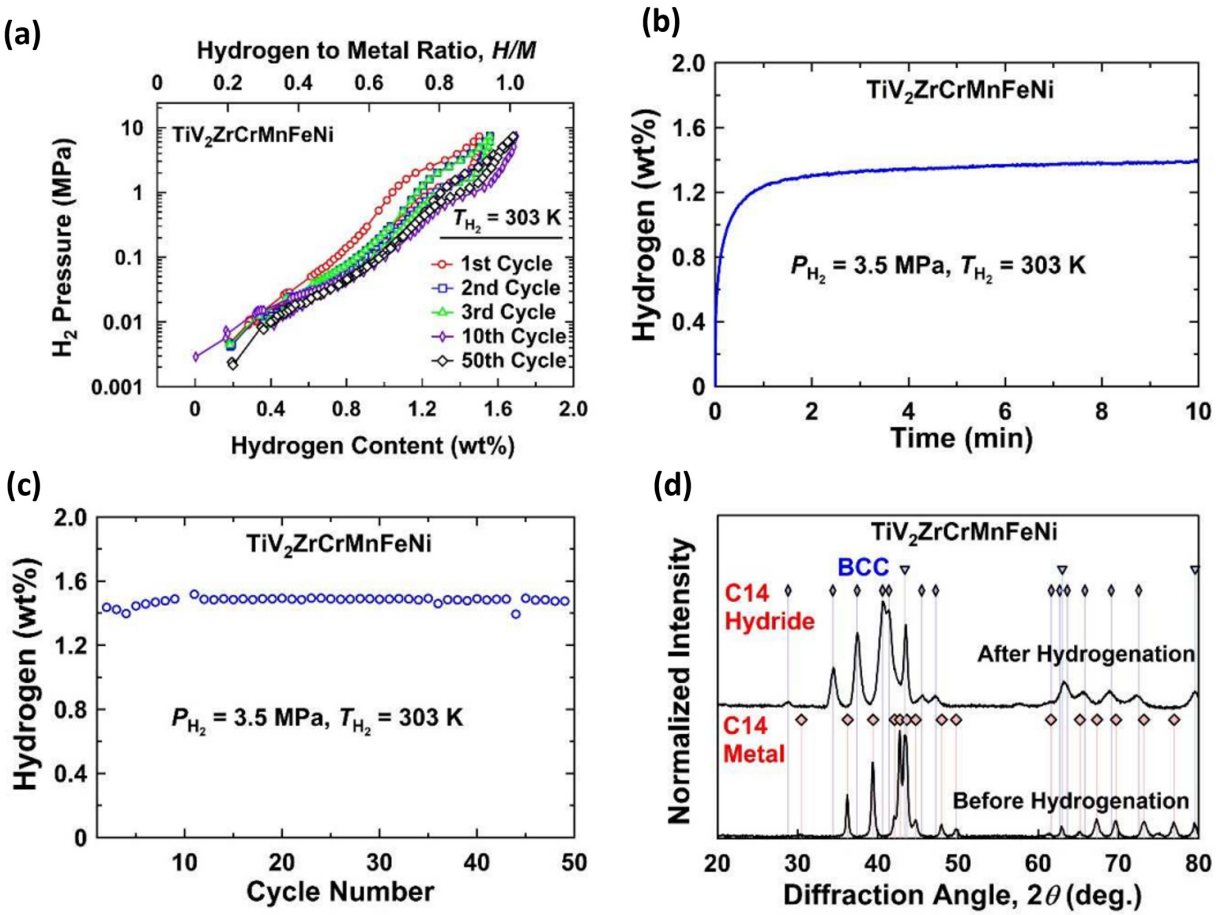


Figure 7. Reversible and quick storage of hydrogen at room temperature in high-entropy alloy $TiV_2ZrCrMnFeNi$ in the form of Laves phase hydride (a = b = 0.519 nm and c = 0.849 nm). (**a**) PCT absorption/desorption isotherms at 303 K, (**b**) hydrogenation kinetics curve at 303 K (blue line represents hydrogen uptake as a function of time), (**c**) hydrogenation cycling tests for 50 cycles at 303 K (circles represent experimental cycling data), and (**d**) XRD profile before and after hydrogenation, where symbols indicate diffraction peak positions corresponding to the identified phases. Reprinted from Ref. [124].

In situ synchrotron and neutron diffraction techniques play a particularly important role in understanding hydrogen-induced phase transformations in HEAs. For example, Glazyrin and co-workers investigated the Cantor alloy CoCrFeNiMn under high-pressure

and high-temperature conditions, where in situ XRD revealed the formation of an FCC hydride phase accompanied by shifts in diffraction peaks toward lower 2θ angles, corresponding to lattice expansion caused by hydrogen incorporation into interstitial sites [125]. Simultaneously, broadening of the XRD peaks indicated the development of microstrains and local structural distortions after hydrogenation, as illustrated in Figure 8b. These results demonstrate that high-pressure/high-temperature processing can induce substantial reconstruction of the crystal structure and significantly alter the thermodynamic stability of hydride phases.

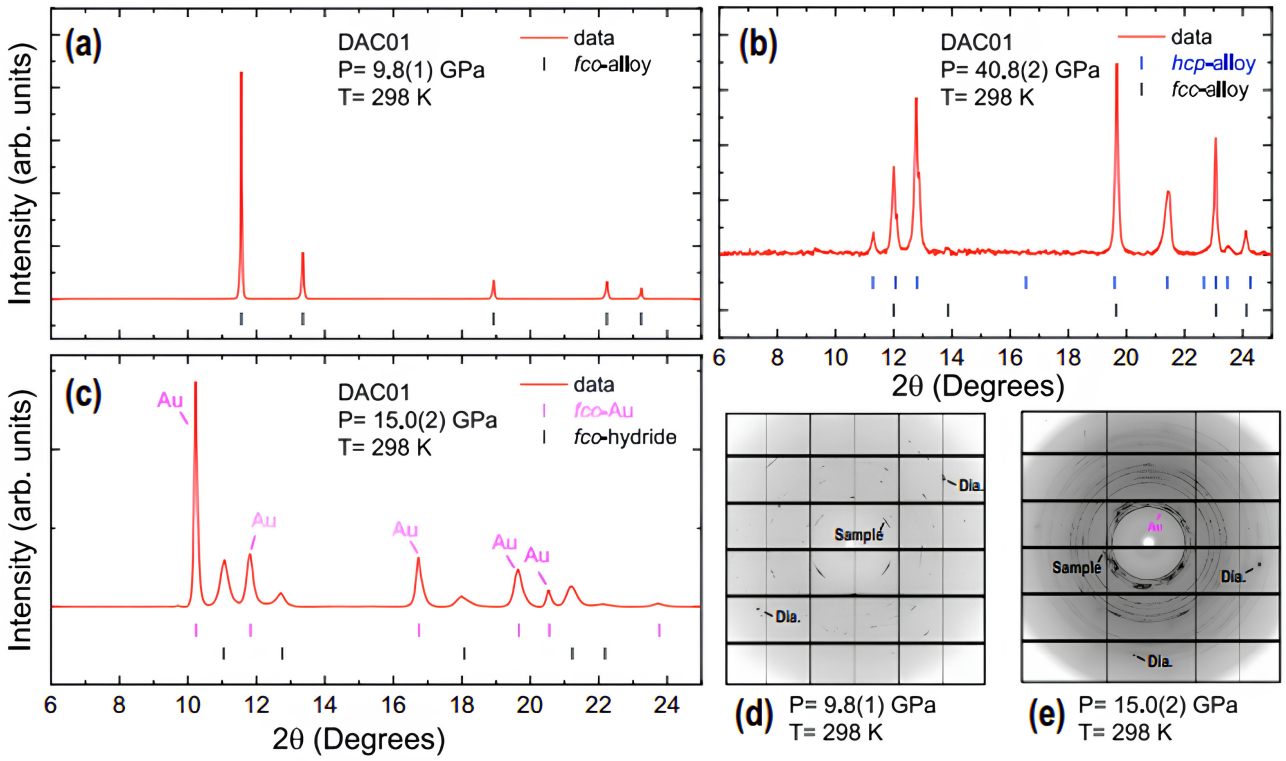


Figure 8. In situ powder XRD patterns of the DAC01 high-entropy alloy during hydrogenation under pressure: (**a**) initial FCC alloy at 9.8 GPa; (**b**) sample after heating at 40.8 GPa with formation of an HCP phase; (**c**) hydride phase after cooling at 15 GPa; and (**d**,**e**) corresponding micrographs of the sample investigated in a diamond anvil cell (DAC). Reprinted from Ref. [125].

Additional insight into surface-related hydrogen interaction mechanisms is provided by XPS and FTIR studies. For CoNiFeCr, CoNiFeV, and CoNiFe(Cr/V) systems synthesized by arc melting, XPS analysis revealed changes in the chemical states of Co, Ni, Fe, Cr, and V after hydrogen evolution reaction (HER) processes, indicating redistribution of electron density and modification of active surface sites (Figure 9a–f). Similarly, FTIR spectroscopy of the CoNiCuRuPd/TiO_2 HEA demonstrated a shift in adsorbed CO bands toward lower wavenumbers, suggesting enhanced electronic interaction between the HEA surface and adsorbates (Figure 9g,h).

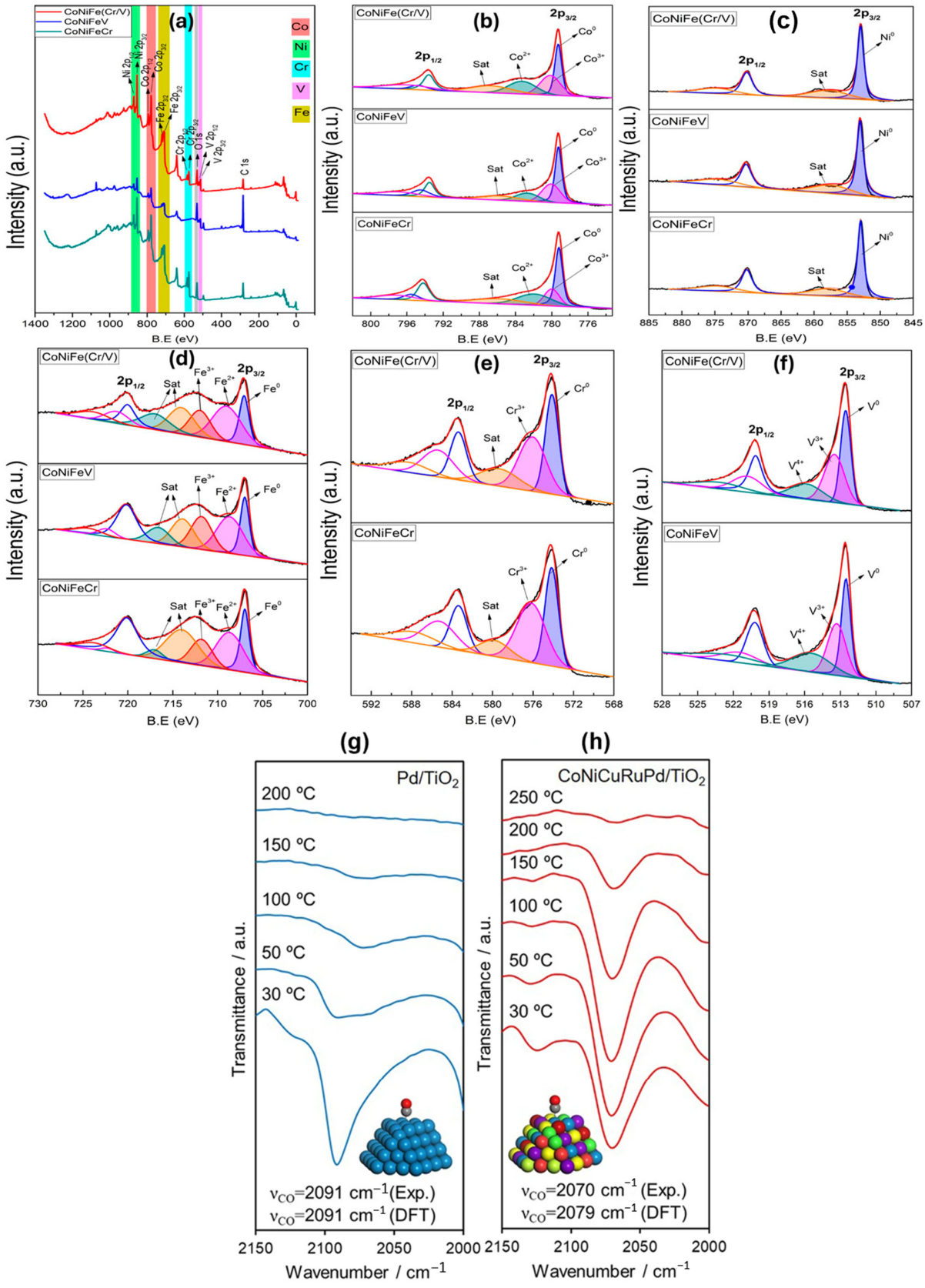


Figure 9. XPS plots of CoNiFeCr, CoNiFeV, and CoNiFe(Cr/V) HEA samples. (**a**) Survey scan. High resolution elemental spectra of (**b**) Co2p, (**c**) Ni2p, (**d**) Fe2p, (**e**) Cr2p, and (**f**) V2p. Reprinted from Ref. [126]. FTIR data obtained during the TPD of adsorbed CO on (**g**) Pd/TiO2 and (**h**) CoNiCuRuPd/TiO_2. Reprinted from Ref. [127].

6. Thermodynamics, Kinetics, and the Problem of Record Capacities

In studies on HEA hydrides, high hydrogen capacity alone is not sufficient to determine the practical applicability of a material [128,129]. Real-world applications simultaneously require reasonable desorption temperatures, appropriate equilibrium pressures, rapid response kinetics, minimal degradation during cycling, and scalable synthesis routes. Reviews published in 2025 indicate that even the best reported performances still fail to fully satisfy the DOE requirements for onboard hydrogen storage, while the major unresolved challenges remain activation requirements, sluggish kinetics in certain systems, and limited cycling stability [130,131].

In BCC alloys, the principal limitation is often associated with excessive hydride stability [130,131]. A strong tendency toward hydride formation facilitates rapid hydrogen uptake, yet may significantly hinder hydrogen release. Consequently, a fundamental trade-off emerges: increasing the H/M ratio and gravimetric capacity almost inevitably alters the thermodynamic operating window. Therefore, meaningful comparison of newly developed materials requires not only reporting maximum hydrogen capacity but also constructing PCT isotherms, evaluating hydride formation enthalpy and entropy, and analyzing hysteresis behavior [132–134].

An additional complication arises from the fact that the distribution of interstitial site energies in HEAs is typically broader than in binary or ternary alloys. As a result, PCT isotherms may become broadened, plateau regions poorly defined, and direct application of conventional van't Hoff analysis less straightforward [116,117]. Under such conditions, in situ/operando techniques, synchrotron XRD, neutron diffraction, local electron microscopy, and atomistic modeling become particularly valuable. The integration of these approaches appears to be the most reliable strategy for correlating macroscopic PCT data with local structural evolution [135].

Finally, the comparability of experimental protocols must also be carefully considered. Hydrogen capacities measured after intensive mechanical activation and repeated high-pressure activation procedures are not directly equivalent to those obtained for cast materials tested under mild conditions. Similarly, room-temperature absorption measured at 3 MPa H2 cannot be directly compared with values obtained at 50 °C or 150 °C [136]. This issue is especially critical for HEA hydrides because microstructure and surface state strongly influence sorption behavior. Therefore, one of the most important challenges for the coming years is the standardization of measurement protocols and reporting methodologies [137].

7. Computational Design: CALPHAD, DFT, and Machine Learning

The vast compositional space of HEAs makes purely empirical exploration highly inefficient. Even when considering only five to seven elements with several concentration levels, the number of possible compositions becomes enormous. Consequently, computational approaches play an increasingly important role in the design of multicomponent hydride-forming systems. The CALPHAD method is one of the key thermodynamic tools for predicting phase equilibria and constructing phase diagrams in multicomponent systems, making it particularly valuable for HEA design [138]. It enables evaluation of the influence of elemental ratios on phase stability, prediction of alloy structures, and optimization of compositions prior to experimental synthesis. In practice, this approach is implemented through software packages such as FactSage and Thermo-Calc, which are especially востребованы for HEAs because of the complexity of interelement interactions in multicomponent systems [139–142].

When designing HEAs, particularly BCC systems, it is essential to consider the solubility of all constituent elements, since limited solid solubility may hinder both melting

and formation of homogeneous alloys [143]. CALPHAD calculations have been shown to predict phase constitution and stability regions of single-phase structures with reasonable accuracy. In several studies, the calculations were in good agreement with experimental observations, allowing identification of stability ranges for BCC and Laves phases and prediction of secondary-phase precipitation during cooling [144–146]. Such information is particularly important for selecting synthesis conditions, including the need for rapid cooling to preserve target single-phase structures.

For lightweight HEAs, additional caution is required when applying CALPHAD because low-melting elements such as Mg or Al may lead to mass loss, compositional deviations, and discrepancies between predicted and actual phase states [147]. Moreover, the incorporation of lightweight hydride-forming elements alone does not guarantee high hydrogen capacity, since sorption behavior depends on a complex interplay of phase constitution, local chemistry, and thermodynamic stability. It should also be noted that the predictive accuracy of CALPHAD strongly depends on the completeness and quality of thermodynamic databases. Although the method possesses high predictive value, its applicability remains limited by insufficient descriptions of multicomponent systems, the complexity of interelement interactions, and the influence of real thermal-processing conditions [142,148,149]. Nevertheless, modern databases such as TCHEA significantly expand the capabilities of computational HEA design by providing Gibbs energy descriptions for a broad range of phases and enabling prediction of both stable and metastable states [144].

DFT and related atomistic approaches provide the next level of insight. These methods allow evaluation of hydrogen energetics in tetrahedral and octahedral interstitial sites, modeling of BCC→BCT/FCC transformations, analysis of alloying-element effects on hydride stability, and even prediction of hydrogen-induced changes in vacancy behavior and mechanical properties [150–152]. Studies on TiZrVMoNb, NbTiVZr, and TiZrNbHfTa demonstrate that without atomistic modeling, it is difficult to adequately interpret observed phase transformations and interstitial occupation sequences [153,154].

In modern materials science, computational databases have become essential tools for analysis, prediction, and discovery of materials with targeted properties. However, reliance solely on databases and expert intuition may result in overlooking potentially promising high-performance systems [155]. Therefore, data-driven materials science, based on data mining, machine learning, and mathematical optimization, is playing an increasingly important role [156,157]. Such approaches aim to identify relationships among composition, structure, and properties, which is particularly valuable for the development of hydrogen storage alloys. High-throughput screening and machine-learning techniques significantly accelerate the search for optimal materials and enable exploration beyond previously known compositions and structural motifs [158–162]. This reduces dependence on lengthy trial-and-error experimentation and makes alloy design more targeted and cost-effective.

For example, Suwarno et al. [163] constructed a database of 314 AB2-type alloys containing information on composition, hydrogen absorption enthalpy, storage capacity, and related properties. Using multiple linear regression, decision trees, and random forest models, they demonstrated that increasing Ni content decreases hydride formation enthalpy, increasing Zr stabilizes the C14 phase while destabilizing C15, and Mn positively affects hydrogen capacity within a certain compositional range. The authors also found that the highest hydrogen capacity is achieved near compositions close to ABx ($1.9 \leq x \leq 2.0$).

In another study, Kim et al. [164] compiled a dataset of 33 alloys and applied random forest, k-nearest neighbors, and deep neural network (DNN) models to predict PCT curves. The DNN model showed the highest accuracy and strong agreement between calculated and experimental data, confirming the promise of deep-learning approaches for describing hydride thermodynamics. Similarly, Lu et al. [165] used a dataset of 81 V-Ti-Cr-Fe alloys

containing 19 structural descriptors to predict hydrogen capacity through an ensemble of six machine-learning models. Despite the limited test dataset, deviations between predicted and experimental capacities were only 0.02–0.04 wt.% H_2, demonstrating high predictive accuracy, although the authors emphasized the need for larger databases to improve model generalization.

For the design of novel HEAs, Witman et al. [166] improved regression and classification models based on gradient boosting by expanding both feature sets and training data, enabling efficient screening of hundreds of candidate materials. Their approach allowed prediction of hydride formation enthalpy and improved identification of promising alloy compositions. Another study on AB5 alloys [167] showed that atomic radius, lattice parameter, and crystal structure type are among the most important factors controlling hydrogen storage behavior, indicating that sorption properties depend not only on composition but also on a combination of structural and thermodynamic parameters.

Despite the considerable progress of computational approaches, none of them can yet be regarded as a universal design tool for HEA hydrides. CALPHAD effectively describes phase equilibria and thermodynamic stability regions, but its accuracy strongly depends on the completeness of thermodynamic databases [139]. As noted by Bengt Hallstedt et al., the predictive capability of CALPHAD for multicomponent systems remains limited by insufficient thermodynamic descriptions and the lack of experimental data for complex concentrated alloys [168]. Additional difficulties arise when modeling hydrogen-containing phases, locally heterogeneous states, and metastable structures characteristic of HEA hydrides [57].

DFT modeling provides a deeper understanding of interstitial energetics, electronic structure, and phase transformation mechanisms [169]. However, computational complexity increases sharply with the number of alloying elements, the degree of chemical disorder, and the supercell size. Moreover, most DFT studies are performed for idealized structures and do not fully account for defects, segregation, residual stresses, or kinetic effects present in real materials [10]. As demonstrated for TiZrNbHfTa systems, broad distributions of local interstitial energies significantly complicate direct comparison between theoretical predictions and experimental observations [30].

Machine-learning methods possess considerable potential for accelerated compositional screening, yet their reliability and transferability remain limited [166]. The main challenge arises from the relatively small amount of available experimental data, differences in testing protocols, incomplete microstructural descriptions, and the lack of standardization of PCT characteristics. As a result, many models demonstrate high accuracy within the training dataset but lose predictive capability when extrapolated to new compositional regions [163]. Another important limitation is that many ML approaches identify statistical correlations without directly revealing the underlying physical mechanisms of hydride formation [157].

Thus, machine-learning approaches are becoming increasingly important tools in the development of hydrogen storage materials, including HEAs. However, achieving truly reliable and transferable predictions will require further accumulation, standardization, and integration of thermodynamic, structural, kinetic, and cyclic data for both alloys and their hydrides. The development of scalable and physically interpretable databases, together with the integration of CALPHAD, DFT, in situ/operando characterization, and physically informed machine learning, appears to be a key prerequisite for transitioning from empirical alloy discovery toward truly predictive design of hydrogen storage materials.

8. Unresolved Problems and Future Prospects

Despite the rapid growth of research on HEA hydrides, many aspects of their practical application and fundamental understanding remain insufficiently explored. One of the major unresolved challenges is achieving a balance among three parameters that rarely improve simultaneously: high hydrogen capacity, favorable desorption thermodynamics, and long-term cyclic stability. In many systems, improvement of one property is accompanied by deterioration of others [170–172]. As illustrated in Figure 10, HEAs possess several characteristics that make them attractive for hydrogen storage applications, including the possibility of tailoring phase constitution and hydrogen sorption behavior. At the same time, their practical implementation remains constrained by the limited understanding of fundamental hydrogen–material interaction mechanisms, the complexity of multicomponent compositions, kinetic limitations, the requirement for elevated operating temperatures in some systems, and the high cost of certain alloying elements.

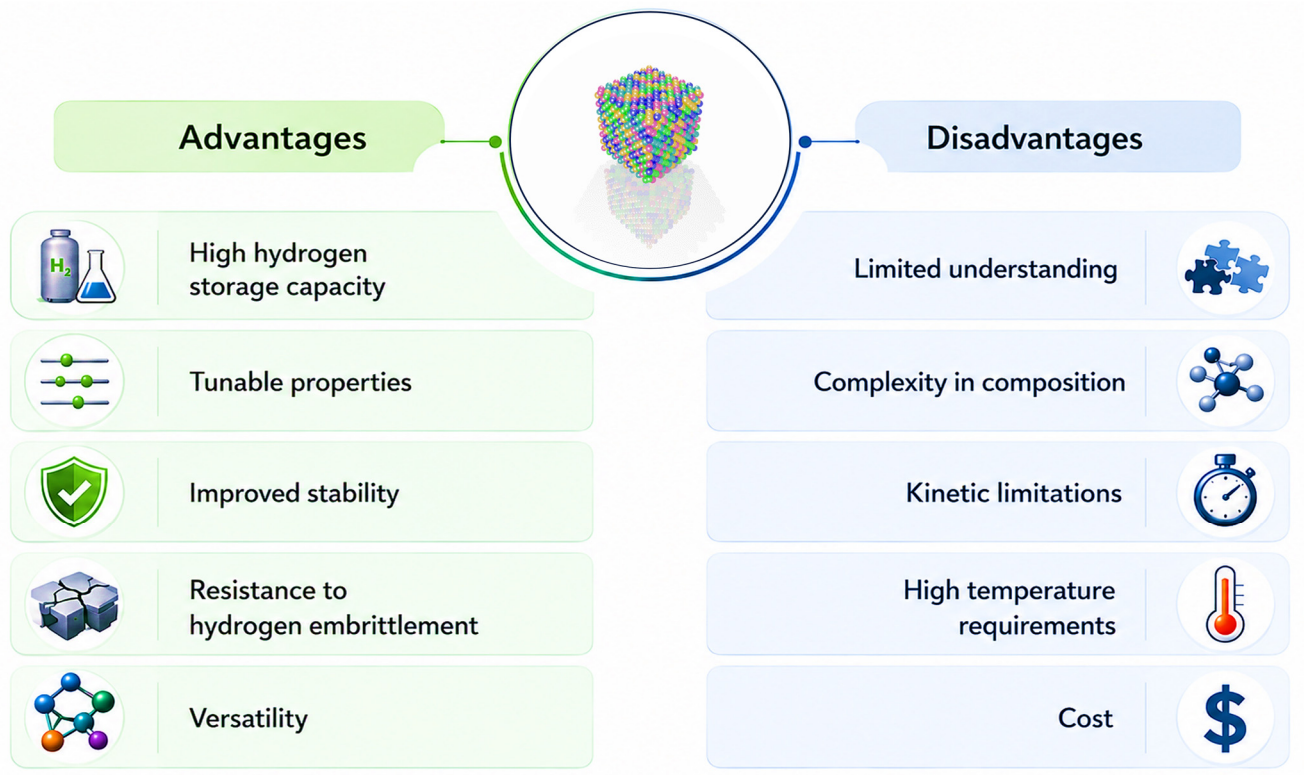


Figure 10. Schematic comparison of the key advantages and limitations of high-entropy alloys as hydrogen storage materials.

The second major challenge is activation. Although room-temperature activation without thermal pretreatment has already been demonstrated for several alloys, a significant number of systems still depend on specific processing histories, hydrogen-induced cracking, or alloying additives to achieve effective hydrogen uptake [173,174]. From a practical standpoint, the ability to activate a material under mild temperature and pressure conditions without complex pretreatment procedures remains a critical requirement [175].

The third challenge concerns cyclic durability. In many studies, the number of investigated hydrogenation/dehydrogenation cycles remains limited, making a reliable assessment of long-term material stability difficult. Comprehensive long-term investigations involving hundreds or thousands of cycles are required, together with simultaneous analysis of phase evolution, particle refinement, intergranular cracking, thermal conductivity, and retained reversible capacity [176]. The lack of such systematic studies currently limits objective comparison of materials in terms of their practical applicability [177,178].

The fourth issue relates to the conceptual boundaries of HEAs for hydrogen storage. Promising candidates are represented not only by classical equiatomic HEAs, but also by a broader range of compositionally complex systems, including non-equiatomic BCC alloys and multicomponent Laves phases [179]. Therefore, future progress in the field is likely to depend on broadening this conceptual framework rather than rigid adherence to the original definitions of HEAs [180].

A promising strategy for the design of HEA hydrides may involve the following stages: (i) physically informed compositional pre-screening; (ii) CALPHAD-based evaluation of phase stability windows; (iii) DFT analysis of local interstitial chemistry and hydrogen-induced transformations; (iv) targeted synthesis with controlled microstructure; (v) standardized PCT and kinetic testing; (vi) in situ/operando characterization combined with cyclic stability studies; and (vii) reintegration of experimental data into machine-learning and thermodynamic databases. Integration of experimental and computational approaches may substantially improve the efficiency of rational design of novel HEA-based hydrogen storage materials [181–185].

9. Conclusions

HEAs and compositionally complex alloys represent a promising class of materials for solid-state hydrogen storage owing to their broad capability for tuning phase constitution, local chemistry, defect structure, and hydride thermodynamics. In contrast to conventional hydride systems, multicomponent HEAs provide a much wider range of structural states and interstitial configurations, thereby offering additional opportunities for controlling hydrogen sorption behavior.

It has been demonstrated that the hydrogen storage performance of HEAs is governed by a complex interplay of factors, including crystal structure type, phase constitution, local chemical heterogeneity, distribution of interstitial site energies, defect structure, and processing route. Among the most promising systems for hydrogen storage are BCC-dominant Ti-V-Zr-Nb-based alloys and multicomponent Laves phases, which are capable of providing a favorable balance among hydrogen capacity, reversibility, and desorption conditions. At the same time, high hydrogen capacity alone is not a sufficient criterion for practical applicability, since kinetics, cyclic stability, activation behavior, and reproducibility are equally important.

Analysis of recent studies indicates that traditional empirical descriptors, including VEC, δ, Ω, and ΔH_{mix}, remain valuable for preliminary compositional screening; however, their predictive capability is limited by the complex local chemistry and energetic heterogeneity of multicomponent systems. Consequently, further progress in the field increasingly relies on integration of computational and experimental approaches, including CALPHAD modeling, DFT calculations, machine-learning methods, and in situ/operando characterization.

Despite significant advances, HEA hydrides still face several fundamental and practical limitations, including the challenge of balancing high hydrogen capacity with favorable desorption thermodynamics, ensuring long-term cyclic stability, standardizing experimental protocols, and expanding reliable databases for hydride-forming systems. Therefore, future progress will depend on the transition from empirical exploration of individual compositions toward physically informed rational design of materials with targeted properties.

Thus, HEA-based hydride systems should not be regarded as universal replacements for conventional hydrogen storage materials, but rather as a flexible platform for developing new functional materials whose properties can be tailored through integrated control of composition, structure, and microstructure. The integration of advanced computational design methods, high-precision structural characterization, and standardized evaluation

protocols for hydrogen sorption behavior represents one of the most promising directions for the future development of materials for hydrogen energy applications.

Author Contributions: Conceptualization, S.K., M.S. and T.K.; methodology, S.R., A.T. and Y.D.; investigation, S.R., T.K., Y.A., A.T. and Y.D.; formal analysis, A.T. and Y.D.; data curation, Y.D.; visualization, S.K., S.R. and Y.A.; writing—original draft preparation, S.K., T.K., Y.A. and M.S.; writing—review and editing, M.S., S.K., T.K. and Y.A.; project administration, S.K. and M.S.; funding acquisition, M.S., Y.A. and S.K. All authors have read and agreed to the published version of the manuscript.

Funding: This research is funded by the Committee of Science of the Ministry of Science and Higher Education of the Republic of Kazakhstan (Grant No.BR24992854).

Data Availability Statement: The original contributions presented in this study are included in the article. Further inquiries can be directed to the corresponding author.

Acknowledgments: We express our gratitude to the Science Committee of the Ministry of Science and Higher Education of the Republic of Kazakhstan, for support of the project "Development and implementation of competitive science-based technologies to ensure sustainable development of mining and metallurgy industry East Kazakhstan region".

Conflicts of Interest: The authors declare no conflicts of interest.

References

1. Kozhakhmetov, Y.; Skakov, M.; Kurbanbekov, S.; Uazyrkhanova, G.; Kurmantayev, A.; Kizatov, A.; Mussakhan, N. High-entropy alloys: Innovative materials with unique properties for hydrogen storage and technologies for their production. *Metals* **2025**, *15*, 100. [CrossRef]
2. Nygård, M.M.; Fjellvåg, Ø.S.; Sørby, M.H.; Sakaki, K.; Ikeda, K.; Armstrong, J.; Vajeeston, P.; Sławiński, W.A.; Kim, H.; Machida, A.; et al. The average and local structure of TiVCrNbDx (x = 0, 2.2, 8) from total scattering and neutron spectroscopy. *Acta Mater.* **2020**, *205*, 116496. [CrossRef]
3. Zareipour, F.; Shahmir, H.; Huang, Y.; Patel, A.K.; Dematteis, E.M.; Baricco, M. Hydrogen storage in TiVCr(Fe, Co)(Zr, Ta) multi-phase high-entropy alloys. *Int. J. Hydrogen Energy* **2024**, *94*, 639–649. [CrossRef]
4. Ichii, K.; Koyama, M.; Tasan, C.C.; Tsuzaki, K. Comparative study of hydrogen embrittlement in stable and metastable high-entropy alloys. *Scr. Mater.* **2018**, *150*, 74–77. [CrossRef]
5. Montero, J.; Ek, G.; Sahlberg, M.; Zlotea, C. Improving the hydrogen cycling properties by Mg addition in Ti-V-Zr-Nb refractory high entropy alloy. *Scr. Mater.* **2021**, *194*, 113699. [CrossRef]
6. Qureshi, T.; Khan, M.M.; Pali, H.S. The future of hydrogen economy: Role of high-entropy alloys in hydrogen storage. *J. Alloys Compd.* **2024**, *1004*, 175668. [CrossRef]
7. George, E.P.; Raabe, D.; Ritchie, R.O. High-entropy alloys. *Nat. Rev. Mater.* **2019**, *4*, 515–534. [CrossRef]
8. Dornheim, M. Thermodynamics–interaction studies–solids. *Liq. Gases* **2011**, *932*. [CrossRef]
9. Liang, J.; Li, G.; Ding, X.; Wen, Z.; Zhang, T.; Li, Y.; Qu, Y. Formation of Zr-rich BCC phase and its relation on the hydrogen storage properties of TiVNbZr high entropy alloy. *Int. J. Hydrogen Energy* **2023**, *48*, 33610–33619. [CrossRef]
10. Nygård, M.M.; Ek, G.; Karlsson, D.; Sørby, M.H.; Sahlberg, M.; Hauback, B.C. Counting electrons—A new approach to tailor the hydrogen sorption properties of high-entropy alloys. *Acta Mater.* **2019**, *175*, 121–129. [CrossRef]
11. Dewangan, S.K.; Sharma, V.K.; Sahu, P.; Kumar, V. Synthesis and characterization of hydrogenated novel AlCrFeMnNiW high entropy alloy. *Int. J. Hydrogen Energy* **2020**, *45*, 16984–16991. [CrossRef]
12. Luo, L.; Chen, L.; Li, L.; Liu, S.; Li, Y.; Li, C.; Li, Y. High-entropy alloys for solid hydrogen storage: A review. *Int. J. Hydrogen Energy* **2024**, *50*, 406–430. [CrossRef]
13. Zhang, C.; Wu, Y.; You, L.; Cao, X.; Lu, Z.; Song, X. Investigation on the activation mechanism of hydrogen absorption in TiZrNbTa high entropy alloy. *J. Alloys Compd.* **2019**, *781*, 613–620. [CrossRef]
14. Floriano, R.; Zepon, G.; Edalati, K.; Fontana, G.L.; Mohammadi, A.; Ma, Z.; Contieri, R.J. Hydrogen storage in TiZrNbFeNi high entropy alloys designed by thermodynamic calculations. *Int. J. Hydrogen Energy* **2020**, *45*, 33759–33770. [CrossRef]
15. Wang, Y.; Li, D.; Wang, S.; Zhang, M.; Gong, P.; Hu, Z.; Li, B. Effect of Cr content on the high temperature oxidation behavior of FeCoNiMnCrx porous high-entropy alloys. *J. Mater. Res. Technol.* **2024**, *33*, 3324–3333. [CrossRef]
16. Jiang, Z.; Chen, H.; Niu, M.; Cheng, J. Mechanical properties of CoCrFeNi-X (X = Ti, Sn) high entropy alloy and tribological properties in simulated seawater environment. *Tribol. Int.* **2025**, *202*, 110306.

17. Lian, G.; Gao, W.; Chen, C.; Huang, X.; Feng, M. Review on hard particle reinforced laser cladding high-entropy alloy coatings. *J. Mater. Res. Technol.* **2024**, *33*, 1366–1405. [CrossRef]
18. Gong, J.; Li, Y.; Song, X.; Wang, Y.; Chen, Z. Hydrogen storage of high entropy alloy NbTiVZr and its effect on mechanical properties: A first-principles study. *Vacuum* **2024**, *219*, 112754. [CrossRef]
19. Yeh, J.W.; Chen, S.K.; Lin, S.J.; Gan, J.Y.; Chin, T.S.; Shun, T.T.; Chang, S.Y. Nanostructured high-entropy alloys with multiple principal elements: Novel alloy design concepts and outcomes. *Adv. Eng. Mater.* **2004**, *6*, 299–303. [CrossRef]
20. Cantor, B.; Chang, I.T.H.; Knight, P.; Vincent, A.J.B. Microstructural development in equiatomic multicomponent alloys. *Mater. Sci. Eng. A* **2004**, *375*, 213–218. [CrossRef]
21. He, Q.F.; Ding, Z.Y.; Ye, Y.F.; Yang, Y.C. Design of high-entropy alloy: A perspective from nonideal mixing. *JOM* **2017**, *69*, 2092–2098. [CrossRef]
22. Ren, J.; Musyoka, N.M.; Langmi, H.W.; Mathe, M.; Liao, S. Current research trends and perspectives on materials-based hydrogen storage solutions: A critical review. *Int. J. Hydrogen Energy* **2017**, *42*, 289–311. [CrossRef]
23. Sreedhar, I.; Kamani, K.M.; Kamani, B.M.; Reddy, B.M.; Venugopal, A. A bird's eye view on process and engineering aspects of hydrogen storage. *Renew. Sustain. Energy Rev.* **2018**, *91*, 838–860. [CrossRef]
24. International Energy Agency. *Global Hydrogen Review 2023*; International Energy Agency: Paris, France, 2023.
25. Rajendrachari, S. An overview of high-entropy alloys prepared by mechanical alloying followed by the characterization of their microstructure and various properties. *Alloys* **2022**, *1*, 116–132. [CrossRef]
26. Abe, J.O.; Popoola, A.P.I.; Ajenifuja, E.; Popoola, O.M. Hydrogen energy, economy and storage: Review and recommendation. *Int. J. Hydrogen Energy* **2019**, *44*, 15072–15086. [CrossRef]
27. Yeh, J.W.; Chen, Y.L.; Lin, S.J.; Chen, S.K. High-entropy alloys—A new era of exploitation. *Mater. Sci. Forum* **2007**, *560*, 1–9.
28. Miracle, D.B.; Senkov, O.N. A critical review of high entropy alloys and related concepts. *Acta Mater.* **2017**, *122*, 448–511. [CrossRef]
29. Dangwal, S.; Edalati, K. High-entropy alloy TiV2ZrCrMnFeNi for hydrogen storage at room temperature with full reversibility and good activation. *Scr. Mater.* **2024**, *238*, 115774. [CrossRef]
30. Zlotea, C.; Sow, M.A.; Ek, G.; Couzinié, J.P.; Perrière, L.; Guillot, I.; Bourgon, J.; Møller, K.T.; Jensen, T.R. Hydrogen sorption in TiZrNbHfTa high entropy alloy. *J. Alloys Compd.* **2019**, *775*, 667–674. [CrossRef]
31. Zhang, C.; Song, A.; Yuan, Y.; Wu, Y.; Zhang, P.; Lu, Z.; Song, X. Study on the hydrogen storage properties of a TiZrNbTa high entropy alloy. *Int. J. Hydrogen Energy* **2020**, *45*, 5367–5374. [CrossRef]
32. Wang, Q.; Qin, Y.; Xie, J.; Kong, Y.; Sun, Q.; Wei, Z.; Zhao, S. Size-controllable high-entropy alloys toward stable hydrogen production at industrial-scale current densities. *Adv. Mater.* **2025**, *37*, 2420173. [CrossRef] [PubMed]
33. Wang, Z.J.; Bai, X.Y.; Wang, J.B.; Jiang, H.; Jiao, W.N.; Li, T.X.; Lu, Y.P. A decade review of eutectic high-entropy alloys (2014–2024): Design, preparation and applications. *Acta Metall. Sin.* **2024**, *1*, 17.
34. Fan, X.K.; Wu, B.; Zhao, C.J.; Dai, W.J. New progress in the research on preparation technologies of high-entropy alloys. *Henan Sci.* **2024**, *42*, 1561–1569.
35. Li, Z.J.; Song, J.; Xu, G.Z.; Hao, W.K.; Luo, H. Research progress on brittle behavior of high-entropy metal materials in hydrogen environment. *Surf. Technol.* **2024**, *53*, 321–348.
36. Guo, Z.H.; Liu, M.; Ma, Y.; Yu, H.; Jing, S.R.; Yan, Y. Hydrogen embrittlement and corrosion resistance of NiCoCr-based equimolar face-centered cubic medium-/high-entropy alloys. *Corros. Sci.* **2025**, *245*, 112700. [CrossRef]
37. Koyama, M.; Wang, H.Y.; Verma, V.K.; Tsuzaki, K.; Akiyama, E. Effects of Mn content and grain size on hydrogen embrittlement susceptibility of face-centered cubic high-entropy alloys. *Metall. Mater. Trans. A* **2020**, *51*, 5612–5616. [CrossRef]
38. Zhang, S.D. Study on Hydrogen Embrittlement Resistance of Al-Co-Cr-Fe-Ni High-Entropy Alloys. Master's Thesis, University of Shanghai for Science and Technology, Shanghai, China, 2022; pp. 21–23.
39. Lu, Y.P.; Gao, X.Z.; Jiang, L.; Chen, Z.N.; Wang, T.M.; Jie, J.C.; Kang, H.J.; Zhang, Y.B.; Guo, S.; Ruan, H.H.; et al. Directly cast bulk eutectic and near-eutectic high entropy alloys with balanced strength and ductility in a wide temperature range. *Acta Mater.* **2017**, *124*, 143–150. [CrossRef]
40. Marques, F.; Balcerzak, M.; Winkelmann, F.; Zepon, G.; Felderhoff, M. Review and outlook on high-entropy alloys for hydrogen storage. *Energy Environ. Sci.* **2021**, *14*, 5191–5227. [CrossRef]
41. Moore, C.M.; Wilson, J.A.; Rushton, M.J.D.; Lee, W.E.; Astbury, J.O.; Middleburgh, S.C. Hydrogen accommodation in the TiZrNbHfTa high entropy alloy. *Scr. Mater.* **2022**, *229*, 117832. [CrossRef]
42. Keith, A.; Zlotea, C.; Szilágyi, P.Á. Perspective of interstitial hydrides of high-entropy alloys for vehicular hydrogen storage. *Int. J. Hydrogen Energy* **2024**, *52*, 531–546. [CrossRef]
43. Hu, J.; Shen, H.; Jiang, M.; Gong, H.; Xiao, H.; Liu, Z.; Zu, X. A DFT study of hydrogen storage in high-entropy alloy TiZrHfScMo. *Nanomaterials* **2019**, *9*, 461. [CrossRef]

44. Mohammadi, A.; Ikeda, Y.; Edalati, P.; Mito, M.; Grabowski, B.; Li, H.W.; Edalati, K. High-entropy hydrides for fast and reversible hydrogen storage at room temperature: Binding-energy engineering via first-principles calculations and experiments. *Acta Mater.* **2022**, *236*, 118117. [CrossRef]
45. Singh, S.; Katiyar, N.K.; Goel, S.; Joshi, S.N. Phase prediction and experimental realisation of a new high entropy alloy using machine learning. *Sci. Rep.* **2023**, *13*, 4811. [CrossRef] [PubMed]
46. Feng, R.; Liaw, P.K.; Gao, M.C.; Widom, M. First-principles prediction of high-entropy-alloy stability. *npj Comput. Mater.* **2017**, *3*, 50. [CrossRef]
47. Gao, T.; Gao, J.; Yang, S.; Zhang, L. Data-driven design of novel lightweight refractory high-entropy alloys with superb hardness and corrosion resistance. *npj Comput. Mater.* **2024**, *10*, 256. [CrossRef]
48. Feng, R.; Zhang, C.; Gao, M.C.; Pei, Z.; Zhang, F.; Chen, Y.; Ma, D.; An, K.; Poplawsky, J.D.; Ouyang, L. High-throughput design of high-performance lightweight high-entropy alloys. *Nat. Commun.* **2021**, *12*, 4896. [CrossRef] [PubMed]
49. Kamnis, S.; Delibasis, K. High entropy alloy property predictions using a transformer-based language model. *Sci. Rep.* **2025**, *15*, 11861. [CrossRef]
50. Hsu, W.L.; Tsai, C.W.; Yeh, A.C.; Yeh, J.W. Clarifying the four core effects of high-entropy materials. *Nat. Rev. Chem.* **2024**, *8*, 471–485. [CrossRef]
51. Yang, F.; Wang, J.; Zhang, Y.; Wu, Z.; Zhang, Z.; Zhao, F.; Huot, J.; Novaković, J.G.; Novaković, N. Recent progress on the development of high entropy alloys (HEAs) for solid hydrogen storage: A review. *Int. J. Hydrogen Energy* **2022**, *47*, 11236–11249. [CrossRef]
52. Shahi, R.R.; Gupta, A.K.; Kumari, P. Perspectives of high entropy alloys as hydrogen storage materials. *Int. J. Hydrogen Energy* **2023**, *48*, 21412–21428. [CrossRef]
53. Lai, Q.; Sun, Y.; Wang, T.; Modi, P.; Cazorla, C.; Demirci, U.B.; Ares Fernandez, J.R.; Geardini, F.; Aguey-Zinsou, K.F. Review on high-entropy alloys for hydrogen storage. *Adv. Sustain. Syst.* **2019**, *3*, 1–64.
54. Zepon, G.; Leiva, D.R.; Strozi, R.B.; Bedoch, A.; Figueroa, S.J.A.; Ishikawa, T.T.; Botta, W.J. Hydrogen storage properties of high-entropy alloys. *Int. J. Hydrogen Energy* **2018**, *43*, 1702–1708. [CrossRef]
55. Marques, F.; Pinto, H.C.; Figueroa, S.J.A.; Winkelmann, F.; Felderhoff, M.; Botta, W.J.; Zepon, G. Hydrogen storage behavior of high-entropy alloys. *Int. J. Hydrogen Energy* **2020**, *45*, 19539–19552. [CrossRef]
56. Scarpati, G.; Frasci, E.; Di Ilio, G.; Jannelli, E. A comprehensive review on metal hydrides-based hydrogen storage systems for mobile applications. *J. Energy Storage* **2024**, *102*, 113934. [CrossRef]
57. Sahlberg, M.; Karlsson, D.; Zlotea, C.; Jansson, U. Superior hydrogen storage in high entropy alloys. *Sci. Rep.* **2016**, *6*, 36770. [CrossRef] [PubMed]
58. Nygård, M.M.; Sławiński, W.A.; Ek, G.; Sørby, M.H.; Sahlberg, M.; Keen, D.A.; Hauback, B.C. Structural investigations of hydrogenated high-entropy alloys. *Acta Mater.* **2020**, *199*, 504–513. [CrossRef]
59. Klopčič, N.; Grimmer, I.; Winkler, F.; Sartory, M.; Trattner, A. A review on metal hydride materials for hydrogen storage. *J. Energy Storage* **2023**, *72*, 108456. [CrossRef]
60. Ma, X.; Ding, X.; Chen, R.; Cao, W.; Song, Q. Study on hydrogen storage property of (ZrTiVFe)xAly high-entropy alloys by modifying Al content. *Int. J. Hydrogen Energy* **2022**, *47*, 8409–8418. [CrossRef]
61. Kumar, A.; Yadav, T.P.; Mukhopadhyay, N.K. Notable hydrogen storage in Ti-Zr-V-Cr-Ni high entropy alloy. *Int. J. Hydrogen Energy* **2022**, *47*, 22893–22900. [CrossRef]
62. Liu, B.; Sun, H.; Guo, S.; Hou, Z.; Mu, X.; Xu, L.; Zhao, D. Structure and hydrogen storage properties of AB_2-type (A = Ti, Zr; B = Cr, Mn, Fe, Co, Ni) C14 Laves phase high-entropy alloys. *Intermetallics* **2026**, *188*, 109089. [CrossRef]
63. Zhao, H.; Yao, P.; Zhao, Y.; Zeng, Z.; Xia, C.; Yang, T. Microstructure and hydrogen storage properties of Zr-based AB_2-type high entropy alloys. *J. Alloys Compd.* **2023**, *960*, 170665. [CrossRef]
64. Ma, X.; Ding, X.; Chen, R.; Chen, X.; Song, Q.; Cui, H. Study on microstructure and the hydrogen storage behavior of a TiVZrNbFe high-entropy alloy. *Intermetallics* **2023**, *157*, 107885. [CrossRef]
65. Floriano, R.; Zepon, G.; Edalati, K.; Fontana, G.L.G.; Mohammadi, A.; Ma, Z.; Li, H.W.; Contieri, R.J. Hydrogen storage properties of new A_3B_2-type TiZrNbCrFe high-entropy alloy. *Int. J. Hydrogen Energy* **2021**, *46*, 23757–23766. [CrossRef]
66. Yeh, J.W. Alloy design strategies and future trends in high-entropy alloys. *JOM* **2013**, *65*, 1759–1771. [CrossRef]
67. Zhang, Y.; Zhou, Y.; Lin, J.; Chen, G.; Liaw, P.K. Solid-solution phase formation rules for multi-component alloys. *Adv. Eng. Mater.* **2008**, *10*, 534–538. [CrossRef]
68. Ye, Y.; Wang, Q.; Lu, J.; Liu, C.; Yang, Y. Design of high entropy alloys: A single-parameter thermodynamic rule. *Scr. Mater.* **2015**, *104*, 53–55. [CrossRef]
69. Yang, X.; Zhang, Y. Prediction of high-entropy stabilized solid-solution in multi-component alloys. *Mater. Chem. Phys.* **2012**, *132*, 233–238. [CrossRef]
70. King, D.; Middleburgh, S.; McGregor, A.; Cortie, M. Predicting the formation and stability of single phase high-entropy alloys. *Acta Mater.* **2016**, *104*, 172–179. [CrossRef]

71. Poletti, M.; Battezzati, L. Electronic and thermodynamic criteria for the occurrence of high entropy alloys in metallic systems. *Acta Mater.* **2014**, *75*, 297–306. [CrossRef]
72. Fang, S.; Xiao, X.; Xia, L.; Li, W.; Dong, Y. Relationship between the widths of supercooled liquid regions and bond parameters of Mg-based bulk metallic glasses. *J. Non-Cryst. Solids* **2003**, *321*, 120–125. [CrossRef]
73. Guo, S.; Liu, C. Phase stability in high entropy alloys: Formation of solid-solution phase or amorphous phase. *Prog. Nat. Sci. Mater. Int.* **2011**, *21*, 433–446. [CrossRef]
74. Guo, S.; Ng, C.; Lu, J.; Liu, C. Effect of valence electron concentration on stability of FCC or BCC phase in high entropy alloys. *J. Appl. Phys.* **2011**, *109*, 103505. [CrossRef]
75. Wu, S.; Wang, D.; Wang, N.; Ma, X.; Xu, Z.; Li, L.; Han, M.; Zhang, C. Compositional design of high-entropy alloys: Advances in structural and hydrogen storage materials. *Alloys* **2026**, *5*, 3. [CrossRef]
76. Miracle, D.B. High entropy alloys as a bold step forward in alloy development. *Nat. Commun.* **2019**, *10*, 1805. [CrossRef] [PubMed]
77. Ramatsoma, B.S.; Makhatha, M.E.; Klenam, D.E.P.; Bodunrin, M.O. Role of compositionally complex and high entropy alloys for hydrogen storage: A bibliometric and mechanistic assessment. *Renew. Sustain. Energy Rev.* **2025**, *222*, 115903. [CrossRef]
78. Lenis, J.A.; Velandia, J.A.; Ocampo, R.A.; Gil, A.A.; Bello, S.; Correa, E.; Arrieta, C.; Bolívar, F.J. Challenges and potential future trends on high entropy alloy for solid hydrogen storage: Systematic review. *J. Power Sources* **2025**, *656*, 238011. [CrossRef]
79. Tarasov, B.P.; Bocharnikov, M.S.; Yanenko, Y.B.; Fursikov, P.V.; Minko, K.B.; Lototskyy, M.V. Metal hydride hydrogen compressors for energy storage systems: Layout features and results of long-term tests. *J. Phys. Energy* **2020**, *2*, 024005. [CrossRef]
80. Dematteis, E.M.; Berti, N.; Cuevas, F.; Latroche, M.; Baricco, M. Substitutional effects in TiFe for hydrogen storage: A comprehensive review. *Mater. Adv.* **2021**, *2*, 2524–2560. [CrossRef]
81. Yang, X.; Li, W.; Zhang, J.; Hou, Q. Hydrogen storage performance of Mg/MgH_2 and its improvement measures: Research progress and trends. *Materials* **2023**, *16*, 1587. [CrossRef]
82. Orimo, S.-I.; Nakamori, Y.; Eliseo, J.R.; Züttel, A.; Jensen, C.M. Complex hydrides for hydrogen storage. *Chem. Rev.* **2007**, *107*, 4111–4132. [CrossRef]
83. Seo, C.Y.; Kim, J.H.; Lee, P.S.; Lee, J.Y. Hydrogen storage properties of vanadium-based BCC solid solution metal hydrides. *J. Alloys Compd.* **2003**, *348*, 252–257. [CrossRef]
84. Dillon, A.C.; Jones, K.M.; Bekkedahl, T.A.; Kiang, C.H.; Bethune, D.S.; Heben, M.J. Storage of hydrogen in single-walled carbon nanotubes. *Nature* **1997**, *386*, 377–379. [CrossRef]
85. Darkrim, F.L.; Malbrunot, P.; Tartaglia, G.P. Review of hydrogen storage by adsorption in carbon nanotubes. *Int. J. Hydrogen Energy* **2002**, *27*, 193–202. [CrossRef]
86. Broom, D.P.; Webb, C.J.; Hurst, K.E.; Parilla, P.A.; Gennett, T.; Brown, C.M.; Zacharia, R.; Tylianakis, E.; Klontzas, E.; Froudakis, G.E.; et al. Outlook and challenges for hydrogen storage in nanoporous materials. *Appl. Phys. A* **2016**, *122*, 151. [CrossRef]
87. Schlapbach, L.; Züttel, A. Hydrogen-storage materials for mobile applications. *Nature* **2001**, *414*, 353–358. [CrossRef]
88. Tozzini, V.; Pellegrini, V. Prospects for hydrogen storage in graphene. *Phys. Chem. Chem. Phys.* **2013**, *15*, 80–89. [CrossRef]
89. Pineda Romero, N.; Zlotea, C.; Marcus, K. High-entropy alloys for hydrogen storage. In *Hydrogen Storage: A Wide Range of Solutions*; de Rango, P., Cuevas, F., Eds.; ISTE Ltd.: London, UK, 2025; pp. 255–301.
90. Shen, S.; Li, Y.; Ouyang, L.; Zhang, L.; Zhu, M.; Liu, Z. V–Ti-based solid solution alloys for solid-state hydrogen storage. *Nano-Micro Lett.* **2025**, *17*, 175. [CrossRef]
91. Jeyaraman, S.; Danilov, D.L.; Notten, P.H.L.; Balachandran, M.; Manivasagam, T.G. Promising hydrogen absorption at room temperature in a magnesium-based high-entropy alloy. *Int. J. Hydrogen Energy* **2026**, *223*, 154245. [CrossRef]
92. Wen, Z.; Wang, S.; Li, Y.; Zhang, T.; Ding, X.; Qu, Y. Effect of Zr content on hydrogen absorption and desorption of TiVCrNb-based high-entropy alloy. *Int. J. Hydrogen Energy* **2025**, *175*, 151468. [CrossRef]
93. Jeyaraman, S.; Danilov, D.L.; Notten, P.H.L.; Ragula, U.B.R.; Ramalingam, V.V.; Manivasagam, T.G. Influence of Ni and Nb addition in TiVCr-based high entropy alloys for room-temperature hydrogen storage. *Energies* **2025**, *18*, 3920. [CrossRef]
94. Liu, J.; Huang, P.; Xia, Y.; Liu, Y.; Luo, Y.; Zhang, H.; Zou, Y.; Chu, H.; Verevkin, S.P. High-entropy alloys for hydrogen storage, separation, and detection: Recent progress and perspectives. *eScience* **2025**, 100506. [CrossRef]
95. Zhang, L.; Li, X.; Qu, X.; Qin, M.; Que, Z.; Wei, Z.; Guo, C.; Lu, X.; Dong, Y. Powder metallurgy route to ultrafine-grained refractory metals. *Adv. Mater.* **2022**, *35*, 2205807. [CrossRef]
96. Gao, S.; Qi, J.; Jia, K.; Zhang, L.; Wu, F.; Xiao, X. A review of high-entropy alloys for next-generation solid-state hydrogen storage. *Compos. Part B Eng.* **2026**, *312*, 113340. [CrossRef]
97. Somo, T.R.; Lototskyy, M.V.; Yartys, V.A.; Davids, M.W.; Nyamsi, S.N. Hydrogen storage behaviours of high entropy alloys: A review. *J. Energy Storage* **2023**, *73*, 108969. [CrossRef]
98. Kong, L.; Cheng, B.; Wan, D.; Xue, Y. A review on BCC-structured high-entropy alloys for hydrogen storage. *Front. Mater.* **2023**, *10*, 1135864. [CrossRef]
99. Balaji, V.; Jeyapandiarajan, P.; Joel, J.; Anbalagan, A.; Ashwath, P.; Anouncia, S.M.; Batako, A.; Xavior, M.A. Mitigating hydrogen embrittlement in high-entropy alloys: A review. *J. Mater. Res. Technol.* **2024**, *33*, 7681–7697. [CrossRef]

100. Kong, X.; Jiang, H.; Lv, Y.; Xie, W.; Lu, S.; Xu, D. Research progress on the hydrogen embrittlement resistance of high-entropy alloys. *Materials* **2025**, *18*, 2862. [CrossRef] [PubMed]
101. Yu, H.; Díaz, A.; Lu, X.; Sun, B.; Ding, Y.; Koyama, M.; He, J.; Zhou, X.; Oudriss, A.; Feaugas, X.; et al. Hydrogen embrittlement as a conspicuous material challenge—Comprehensive review and future directions. *Chem. Rev.* **2024**, *124*, 6271–6392. [CrossRef] [PubMed]
102. El Aalami, B.; Idrissi, H.; Trabadelo, V. C14-Laves phase high entropy alloys for hydrogen storage: A review. *Mater. Horiz.* **2026**, *13*, 3721–3760. [CrossRef]
103. Hassan, N.O.; Ghais, A.; Ahmed, M.H.M.; Adam, M.; Ahmed, R.; Abdelatti, A.; Klenam, D.E.P.; Bodunrin, M.O.; Koko, A. Density functional theory insights into the structure, electronic and mechanical properties, thermodynamics, and diffusion of high-entropy alloys for hydrogen storage: A review. *Int. J. Hydrogen Energy* **2026**, *217*, 153928. [CrossRef]
104. Adeyoye, A.; Popoola, P.; Popoola, O.; Adeosun, S.; Dada, M. Refractory high-entropy alloys for solid-state hydrogen storage: A computational design review. *Int. J. Hydrogen Energy* **2026**, *205*, 153291. [CrossRef]
105. Somo, T.R.; Modibane, K.D.; Maponya, T.C.; Teffu, D.M. Theoretical hydrogen storage properties of high entropy alloys: A combined DFT and machine learning approach. *Mater. Today Commun.* **2025**, *48*, 113366. [CrossRef]
106. Bouzidi, A.; Laversenne, L.; Nassif, V.; Elkaim, E.; Zlotea, C. Hydrogen storage properties of a new Ti-V-Cr-Zr-Nb high entropy alloy. *Hydrogen* **2022**, *3*, 270–284. [CrossRef]
107. Montero, J.; Ek, G.; Laversenne, L.; Nassif, V.; Sahlberg, M.; Zlotea, C. How 10 at% Al addition in the Ti-V-Zr-Nb high-entropy alloy changes hydrogen sorption properties. *Molecules* **2021**, *26*, 2470. [CrossRef]
108. Greaves, F.; Bouzidi, A.; Perrière, L.; Vaughan, G.; Nassif, V.; Laversenne, L.; Borgschulte, A.; Martins, M.L.; Cheng, Y.; Ramirez-Cuesta, A.J.; et al. Hydrogen induced phase transition in TiZrNbHfV1–xTax high entropy alloys. *J. Phys. Chem. C* **2025**, *129*, 2904–2912. [CrossRef]
109. Zhai, Y.T.; Li, Y.M.; Bolzoni, L.; Kennedy, J.; Yang, F. Effect of heat treatment on microstructural evolution and hydrogen storage performance of as-milled Ti_5+xV_{35}(CrMnFe)$_{60-x}$ (x = 0, 10, 20, 30) high-entropy alloys. *Int. J. Hydrogen Energy* **2024**, *81*, 584–594. [CrossRef]
110. Halpren, E.; Yao, X.; Chen, Z.W.; Singh, C.V. Machine learning assisted design of BCC high entropy alloys for room temperature hydrogen storage. *Acta Mater.* **2024**, *270*, 119841. [CrossRef]
111. Radhika, N.; Niketh, M.S.; Akhil, U.V.; Adediran, A.A.; Jen, T.C. High entropy alloys for hydrogen storage applications. *Results Eng.* **2024**, *23*, 102780. [CrossRef]
112. Elharrak, A.; Ait Ousaleh, H.; Mehmood, S.; Bürger, I.; Linder, M.; Faik, A. An analytical review of recent advancements on solid-state hydrogen storage. *Int. J. Hydrogen Energy* **2024**, *52*, 1182–1193.
113. Ma, X.; Chen, R.; Gao, X.; Su, Y.; Cui, H. Enhanced hydrogen storage properties of ZrTiVAl1−xFex high-entropy alloys. *RSC Adv.* **2022**, *12*, 11272–11281. [CrossRef]
114. Rong, M.; Zhou, X.; Liu, Y.; Wang, J.; Zhang, H.; Wang, R.; Wang, F. Composition-driven phase regulation and hydrogen storage performance in Ti-V-based multi-principal high-entropy alloys. *J. Alloys Compd.* **2026**, *1062*, 187589. [CrossRef]
115. Li, Z.; Ludwig, A.; Savan, A.; Springer, H.; Raabe, D. Combinatorial metallurgical synthesis and processing of high entropy alloys. *J. Mater. Res.* **2018**, *33*, 3156–3169. [CrossRef]
116. Biesuz, M.; Saunders, T.G.; Veverka, J.; Bortolotti, M.; Vontorová, J.; Vilémová, M.; Reece, M.J. Solidification microstructures of multielement carbides in the high entropy Zr-Nb-Hf-Ta-Cx system produced by arc melting. *Scr. Mater.* **2021**, *203*, 114091. [CrossRef]
117. Hu, Z.Y.; Zhang, Z.H.; Cheng, X.W.; Wang, F.C.; Zhang, Y.F.; Li, S.L. A review of multi-physical fields induced phenomena and effects in spark plasma sintering: Fundamentals and applications. *Mater. Des.* **2020**, *191*, 108662. [CrossRef]
118. Ding, Z.; Li, Y.; Jiang, H.; Zhou, Y.; Wan, H.; Qiu, J.; Jiang, F.; Tan, J.; Du, W.; Chen, Y.; et al. The integral role of high-entropy alloys in advancing solid-state hydrogen storage. *Interdiscip. Mater.* **2025**, *4*, 75–108. [CrossRef]
119. Aidarova, M.; Kurbanbekov, S.; Kizatov, A.; Urkunbay, A.; Bayatanova, L.; Rutkowska-Gorczyca, M.; Amangeldiyeva, Y. Influence of milling time and binder composition on phase evolution in WC-based composite powders fabricated via high-energy ball milling. *Front. Mater.* **2025**, *12*, 1684414. [CrossRef]
120. Xing, Y.; Li, C.; Mu, Y.; Jia, Y.D.; Song, K.K.; Tan, J.; Wang, G.; Zhang, Z.Q.; Yi, J.H.; Eckert, J. Strengthening and deformation mechanism of high-strength CrMnFeCoNi high entropy alloy prepared by powder metallurgy. *J. Mater. Sci. Technol.* **2023**, *132*, 119–131. [CrossRef]
121. Ha, H.; Jung, S.J.; Jeong, S.G.; Kim, R.E.; Park, H.K.; Kim, H.S. Enhancing hydrogen storage kinetics and capacity via particle size modulation in TiZrCrFeMnNi high-entropy alloy. *Int. J. Hydrogen Energy* **2025**, *99*, 1047–1054. [CrossRef]
122. Kunce, I.; Polański, M.; Czujko, T. Microstructures and hydrogen storage properties of LaNiFeVMn alloys. *Int. J. Hydrogen Energy* **2017**, *42*, 27154–27164. [CrossRef]
123. Park, K.B.; Park, J.Y.; Kim, Y.D.; Na, T.W.; Mo, C.B.; Choi, J.I.; Park, H.K. Spark plasma sintering behavior of TaNbHfZrTi high-entropy alloy powder synthesized by hydrogenation-dehydrogenation reaction. *Intermetallics* **2021**, *130*, 107077. [CrossRef]

124. Li, H.; Yang, F.; Wang, G.; Guan, L.; Lai, F.; Zhang, N.; Liu, T. Highly distorted high-entropy alloy aerogels for high-efficiency hydrogen oxidation reaction. *ACS Nano* **2025**, *19*, 14434–14444. [CrossRef] [PubMed]
125. Glazyrin, K.; Spektor, K.; Bykov, M.; Carvalho, P.H.B.; Dong, W.; Körmann, F.; Sano-Furukawa, A.; Hattori, T.; Beyer, D.C.; Sahlberg, M.; et al. Synthesis of high-entropy hydride from the Cantor alloy (fcc–CoCrFeNiMn) at extreme conditions. *Nat. Commun.* **2026**, *17*, 2622. [CrossRef]
126. Nawaz, T.; Ahmad, S.; Abuzaid, W.; Mustafa, F.; Ahmad, W.; El-Khatib, S.; Kaddoura, M.J.; Alami, A.H.; Alawadhi, H. Enhanced electrocatalytic hydrogen evolution with CoNiFe(Cr/V)-based high entropy alloy electrodes. *APL Mater.* **2025**, *13*, 051114. [CrossRef]
127. Mori, K.; Hashimoto, N.; Kamiuchi, N.; Yoshida, H.; Kobayashi, H.; Yamashita, H. Hydrogen spillover-driven synthesis of high-entropy alloy nanoparticles as a robust catalyst for CO_2 hydrogenation. *Nat. Commun.* **2021**, *12*, 3884. [CrossRef] [PubMed]
128. Deng, Y.; Chen, X.; Qi, H.; Feng, S.; Wang, W.; Xie, L.; Sun, G.; Shen, H.; Zu, X.; Xiao, H. The design of Mg–Ti–V–Nb–Cr lightweight high entropy alloys for hydrogen storage. *Int. J. Hydrogen Energy* **2024**, *87*, 1327–1337. [CrossRef]
129. Yadav, Y.K.; Shaz, M.A.; Yadav, T.P. Solid-state hydrogen storage properties of Al–Cu–Fe–Ni–Ti high entropy alloy. *Int. J. Hydrogen Energy* **2025**, *99*, 985–995. [CrossRef]
130. Yadav, Y.K.; Shaz, M.A.; Yadav, T.P. Notable hydrogen storage properties in nanocrystalline Al–Cr–Cu–Fe–Ni high-entropy alloy. *Int. J. Miner. Metall. Mater.* **2025**, *32*, 2723–2732. [CrossRef]
131. Hidayati, R.; Yun, J.H.; Jo, W.J.; Kim, S.; Kim, W.; Ha, H.; Kim, H.S.; Cho, B.; Kim, J.H.; Rhyee, J.-S.; et al. Multi-functional properties of superconducting and hydrogen storage in bulk $TaNb_2HfZrTi$ high-entropy alloys. *Adv. Funct. Mater.* **2026**, *36*, e30408. [CrossRef]
132. Mazloomi, M.; Shahmir, H.; Forghani, F.; Ismail, M. High-throughput calculations to develop high-entropy alloys for hydrogen storage applications. *Int. J. Hydrogen Energy* **2026**, *228*, 154398. [CrossRef]
133. Zhao, Y.M.; Zhang, J.Y.; Liaw, P.K.; Yang, T. Machine learning-based computational design methods for high-entropy alloys. *High Entropy Alloys Mater.* **2025**, *3*, 41–100. [CrossRef]
134. Lu, Z.; Dong, M.; Liu, X.; Lu, Z. High-throughput and data-driven machine learning techniques for discovering high-entropy alloys. *Commun. Mater.* **2024**, *5*, 76.
135. Ha, M.Q.; Nguyen, D.N.; Nguyen, V.C.; Nagata, T.; Chikyow, T.; Kino, H.; Miyake, T.; Denœux, T. Evidence-based recommender system for high-entropy alloys. *Nat. Comput. Sci.* **2021**, *1*, 46–53. [CrossRef] [PubMed]
136. Greaves, F.; Nassif, V.; Alfredsson, M.; Chadwick, A.V. The role of Al addition on the hydrogen sorption properties of TiVZrNbHf high entropy alloy. *Intermetallics* **2026**, *189*, 109119. [CrossRef]
137. Cheng, B.; Kong, L.; Cai, H.; Li, Y.; Zhao, Y.; Wan, D.; Xue, Y. Pushing the boundaries of solid-state hydrogen storage: A refined study on TiVNbCrMo high-entropy alloys. *Int. J. Hydrogen Energy* **2024**, *60*, 282–292. [CrossRef]
138. Guo, L.; Gu, J.; Gong, X.; Ni, S.; Song, M. CALPHAD-aided design of high entropy alloy to achieve high strength via precipitate strengthening. *Sci. China Mater.* **2019**, *63*, 288–299. [CrossRef]
139. Chen, H.; Mao, H.; Chen, Q. Database development and CALPHAD calculations for high entropy alloys: Challenges, strategies, and tips. *Mater. Chem. Phys.* **2018**, *210*, 279–290. [CrossRef]
140. Guruvidyathri, K.; Hari Kumar, K.; Yeh, J.W.; Murty, B. Topologically close-packed phase formation in high entropy alloys: A review of CALPHAD and experimental results. *JOM* **2017**, *69*, 2113–2124. [CrossRef]
141. Gorsse, S.; Tancret, F. Current and emerging practices of CALPHAD toward the development of high entropy alloys and complex concentrated alloys. *J. Mater. Res.* **2018**, *33*, 2899–2923. [CrossRef]
142. Syed Ghazi, S.; Ravi, K. Phase-evolution in high entropy alloys: Role of synthesis route. *Intermetallics* **2016**, *73*, 40–42. [CrossRef]
143. Ruiz-Yi, B.; Bunn, J.; Stasak, D.; Mehta, A.; Besser, M.; Kramer, M.J.; Takeuchi, I.; Hattrick-Simpers, J. The different roles of entropy and solubility in high entropy alloy stability. *ACS Comb. Sci.* **2016**, *18*, 596–603. [CrossRef] [PubMed]
144. Nagase, T.; Todai, M.; Wang, P.; Sun, S.; Nakano, T. Design and development of (Ti,Zr,Hf)-Al based medium entropy alloys and high entropy alloys. *Mater. Chem. Phys.* **2022**, *276*, 125409. [CrossRef]
145. Edalati, P.; Floriano, R.; Mohammadi, A.; Li, Y.; Zepon, G.; Li, H.W.; Edalati, K. Reversible room temperature hydrogen storage in high-entropy alloy TiZrCrMnFeNi. *Scr. Mater.* **2020**, *178*, 387–390. [CrossRef]
146. Liu, P.; Xie, X.; Xu, L.; Li, X.; Liu, T. Hydrogen storage properties of $(Ti_{0.85}Zr_{0.15})_{1.05}Mn_{1.2}Cr_{0.6}V_{0.1}M_{0.1}$ (M = Ni, Fe, Cu) alloys easily activated at room temperature. *Prog. Nat. Sci. Mater. Int.* **2017**, *27*, 652–657. [CrossRef]
147. Guruvidyathri, K.; Murty, B.; Yeh, J.; Hari Kumar, K.C. Gibbs energy-composition plots as a tool for high-entropy alloy design. *J. Alloys Compd.* **2018**, *768*, 358–367. [CrossRef]
148. Senkov, O.; Miller, J.; Miracle, D.; Woodward, C. Accelerated exploration of multi-principal element alloys for structural applications. *Calphad* **2015**, *50*, 32–48. [CrossRef]
149. Mao, H.; Chen, H.; Chen, Q. TCHEA1: A thermodynamic database not limited for "high entropy" alloys. *J. Phase Equilibria Diffus.* **2017**, *38*, 353–368. [CrossRef]

150. Hu, J.; Shen, H.; Jiang, M.; Gong, H.; Xiao, H.; Liu, Z.; Zu, X. A first-principles study of hydrogen storage of high-entropy alloy TiZrVMoNb. *Int. J. Hydrogen Energy* **2021**, *46*, 21050–21058. [CrossRef]
151. Wan, Y.; Wei, W.; Ding, S.; Wu, L.; Qin, H.; Yuan, X. A multi-site synergistic effect in high-entropy alloy for efficient hydrogen evolution. *Adv. Funct. Mater.* **2025**, *35*, 2414554. [CrossRef]
152. Kumar, P.; Singh, V.K.; Singh, S.K. An experimental and theoretical investigation of room-temperature hydrogen storage in TiVNiNb high-entropy alloy. *Mater. Lett.* **2025**, *388*, 138334. [CrossRef]
153. Jiang, M.; Song, A.; Yan, Y.; Feng, W.; Li, H.; Liang, B. Applicability and limitations of hydrogen affinity as a descriptor for designing high-entropy alloys for hydrogen storage. *Chem. Mater.* **2026**, *38*, 3666–3675. [CrossRef]
154. Surya, K.; Sibi, S.P.; Chanda, B.; Jana, P.P. A tool to conjecture hydrogen storage capacity of high-entropy alloys. *Int. J. Hydrogen Energy* **2025**, *148*, 150069. [CrossRef]
155. Hart, G.L.W.; Mueller, T.; Toher, C.; Curtarolo, S. Machine learning for alloys. *Nat. Rev. Mater.* **2021**, *6*, 730–755. [CrossRef]
156. Zhou, P.; Xiao, X.; Zhu, X.; Chen, Y.; Lu, W.; Piao, M.; Cao, Z.; Lu, M.; Fang, F.; Li, Z.; et al. Machine learning enabled customization of performance-oriented hydrogen storage materials for fuel cell systems. *Energy Storage Mater.* **2023**, *63*, 102964. [CrossRef]
157. Butler, K.T.; Davies, D.W.; Cartwright, H.; Isayev, O.; Walsh, A. Machine learning for molecular and materials science. *Nature* **2018**, *559*, 547–555. [CrossRef]
158. Ponsoni, J.; Aranda, V.; Nascimento, T.; Strozi, R.B.; Botta, W.J.; Zepon, G. Design of multicomponent alloys with C14 Laves phase structure for hydrogen storage assisted by computational thermodynamic. *Acta Mater.* **2022**, *240*, 118317. [CrossRef]
159. Huang, E.; Lee, W.J.; Singh, S.; Kumar, P.; Lee, C.-Y.; Lam, T.-N.; Chin, H.-H.; Lin, B.-H.; Liaw, P.K. Machine-learning and high-throughput studies for high-entropy materials. *Mater. Sci. Eng. R Rep.* **2022**, *147*, 100645. [CrossRef]
160. Ferrari, A.; Dutta, B.; Gubaev, K.; Ikeda, Y.; Srinivasan, P.; Grabowski, B.; Körmann, F. Frontiers in atomistic simulations of high entropy alloys. *J. Appl. Phys.* **2020**, *128*, 150901. [CrossRef]
161. Zhou, Z.; Zhou, Y.; He, Q.; Ding, Z.; Li, F.; Yang, Y. Machine learning guided appraisal and exploration of phase design for high entropy alloys. *npj Comput. Mater.* **2019**, *5*, 128. [CrossRef]
162. Qiao, L.; Liu, Y.; Zhu, J. A focused review on machine learning aided high-throughput methods in high entropy alloy. *J. Alloys Compd.* **2021**, *877*, 160295. [CrossRef]
163. Suwarno, S.; Dicky, G.; Suyuthi, A.; Effendi, M.; Witantyo, W.; Noerochim, L.; Ismail, M. Machine learning analysis of alloying element effects on hydrogen storage properties of AB2 metal hydrides. *Int. J. Hydrogen Energy* **2022**, *47*, 11938–11947. [CrossRef]
164. Kim, J.; Ha, T.; Lee, J.; Lee, Y.S.; Shim, J.H. Prediction of pressure composition-temperature curves of AB2-type hydrogen storage alloys by machine learning. *Met. Mater. Int.* **2022**, *29*, 861–869. [CrossRef]
165. Lu, Z.; Wang, J.; Wu, Y.; Guo, X.; Xiao, W. Predicting hydrogen storage capacity of V–Ti–Cr–Fe alloy via ensemble machine learning. *Int. J. Hydrogen Energy* **2022**, *47*, 34583–34593. [CrossRef]
166. Witman, M.; Ek, G.; Ling, S.; Chames, J.; Agarwal, S.; Wong, J.; Allendorf, M.D.; Sahlberg, M.; Stavila, V. Data-driven discovery and synthesis of high entropy alloy hydrides with targeted thermodynamic stability. *Chem. Mater.* **2021**, *33*, 4067–4076. [CrossRef]
167. Panwar, K.; Srivastava, S. On structural model of AB5-type multi-element hydrogen storage alloy. *Int. J. Hydrogen Energy* **2019**, *44*, 30208–30217. [CrossRef]
168. Hallstedt, B.; Broeckmann, C.; Stein, F. Perspectives of computational thermodynamics for high entropy alloys. *J. Phase Equilibria Diffus.* **2021**, *42*, 1–14.
169. Montero, J.; Ek, G.; Hjörvarsson, B. Hydrogen storage properties of high entropy alloys from first-principles calculations. *Acta Mater.* **2021**, *203*, 116496.
170. Mishra, S.; Maiti, S.; Rai, B. Computational property predictions of Ta-Nb-Hf-Zr high-entropy alloys. *Sci. Rep.* **2021**, *11*, 4815. [CrossRef] [PubMed]
171. Pacchioni, G. Designing ductile refractory high-entropy alloys. *Nat. Rev. Mater.* **2025**, *10*, 1. [CrossRef]
172. Ding, J. Order or disorder, that is the question in high-entropy alloys. *Nat. Rev. Mater.* **2026**, *11*, 82–83. [CrossRef]
173. Qiu, Y.; Thomas, S.; Gibson, M.A.; Fraser, H.L.; Birbilis, N. Corrosion of high entropy alloys. *npj Mater. Degrad.* **2017**, *1*, 15. [CrossRef]
174. Luo, H.; Li, Z.; Raabe, D. Hydrogen enhances strength and ductility of an equiatomic high-entropy alloy. *Sci. Rep.* **2017**, *7*, 9892. [CrossRef]
175. Luo, H.; Li, Z.; Lu, W.; Ponge, D.; Raabe, D. Hydrogen embrittlement of an interstitial equimolar high-entropy alloy. *Corros. Sci.* **2018**, *136*, 403–408. [CrossRef]
176. Li, X.; Meng, X. Recent advances on high entropy alloys for electrocatalytic applications. *Int. J. Hydrogen Energy* **2024**, *82*, 1471–1480. [CrossRef]
177. Tsai, M.H.; Yeh, J.W. High-entropy alloys: A critical review. *Mater. Res. Lett.* **2014**, *2*, 107–123. [CrossRef]
178. Zhang, Y.; Zuo, T.T.; Tang, Z.; Gao, M.C.; Dahmen, K.A.; Liaw, P.K.; Lu, Z.P. Microstructures and properties of high-entropy alloys. *Prog. Mater. Sci.* **2014**, *61*, 1–93. [CrossRef]

179. Miracle, D.B.; Miller, J.D.; Senkov, O.N.; Woodward, C.; Uchic, M.D.; Tiley, J. Exploration and development of high entropy alloys for structural applications. *Entropy* **2014**, *16*, 494–525. [CrossRef]
180. Otto, F.; Yang, Y.; Bei, H.; George, E.P. Relative effects of enthalpy and entropy on the phase stability of equiatomic high-entropy alloys. *Acta Mater.* **2013**, *61*, 2628–2638. [CrossRef]
181. Otto, F.; Dlouhy, A.; Somsen, C.; Bei, H.; Eggeler, G.; George, E.P. The influences of temperature and microstructure on the tensile properties of a CoCrFeMnNi high-entropy alloy. *Acta Mater.* **2013**, *61*, 5743–5755. [CrossRef]
182. Pickering, E.J.; Jones, N.G. High-entropy alloys: A critical assessment of their founding principles and future prospects. *Int. Mater. Rev.* **2016**, *61*, 183–202. [CrossRef]
183. Senkov, O.N.; Miracle, D.B.; Chaput, K.J.; Couzinie, J.P. Development and exploration of refractory high entropy alloys: A review. *J. Mater. Res.* **2018**, *33*, 3092–3128. [CrossRef]
184. Oses, C.; Toher, C.; Curtarolo, S. High-entropy ceramics. *Nat. Rev. Mater.* **2020**, *5*, 295–309. [CrossRef]
185. Alobaid, A.; Kamil, M.; Khalil, K.A. Metal hydrides for solid hydrogen storage: Experimental insights, suitability evaluation, and innovative technical considerations for stationary and mobile applications. *Int. J. Hydrogen Energy* **2025**, *128*, 432–456. [CrossRef]

Disclaimer/Publisher's Note: The statements, opinions and data contained in all publications are solely those of the individual author(s) and contributor(s) and not of MDPI and/or the editor(s). MDPI and/or the editor(s) disclaim responsibility for any injury to people or property resulting from any ideas, methods, instructions or products referred to in the content.